The Interpose PUF: Secure PUF Design against State-of-the-Art Machine Learning Attacks

Phuong Ha Nguyen[1]*, Durga Prasad Sahoo[2], Chenglu Jin[1], Kaleel Mahmood[1], Ulrich Rührmair[3] and Marten van Dijk[1]

[1] University of Connecticut, USA
[2] Bosch India (RBEI/ESY), India
[3] Horst Görtz Institute for IT-Security, Ruhr Universität Bochum, Germany

Abstract.
The design of a strong silicon Physical Unclonable Function (PUF) with a rigorous security argument that is also lightweight and reliable has been the fundamental problem in PUF research, since its introduction in 2002. Becker's reliability based CMA-ES attack in CHES 2015 showed that as of yet, no silicon PUF design can solve this fundamental problem. This is due to the attacker's access to repeated measurements (this gives reliability information) of Challenge Response Pairs (CRPs). We are the first to provide a detailed analysis of when the reliability based CMA-ES attack is successful and when it is not applicable. We introduce the Interpose PUF (IPUF) design and show by using reduction type of arguments that the IPUF design is secure against *all* known machine learning (ML) attacks that use CRPs (but no side channel information). We provide simulations and confirm these by experimenting with an FPGA implementation of the IPUF. The IPUF design solves the fundamental open problem for strong silicon PUFs with respect to all state-of-the-art ML attacks.

Keywords: Physically Unclonable Functions (PUFs) · Strong Silicon PUFs · Machine Learning Attacks

1 Introduction

A PUF is a fingerprint of a chip which behaves as a *one-way function* in the following way: it leverages process manufacturing variation to generate a unique function taking "challenges" as input and generating "responses" as output. Silicon PUFs were introduced in 2002 by Gassend et al. [GCvDD02] and are an emerging hardware security primitive in various applications such as device identification, authentication and cryptographic key generation [MV10, KGM+08, YMSD11, BFSK11]. The fundamental open problem of strong silicon PUFs is: How to exploit *silicon manufacturing variations* to realize a *reliable* PUF design that has a rigorous *security argument*[1] and is *lightweight* while offering a large

*The IPUF design (formerly called MXPUF) was first proposed in the e-print, "MXPUF: Secure PUF Design against State-of-the-art Modeling Attacks", by a subset of current author list. However, this paper has significantly more content and new material as compared to the original paper. This paper presents new simulation results for machine learning attacks on a larger range of IPUF configurations and simulation results for the strict avalanche criterion (SAC) property. This paper also presents experimental results for an IPUF FPGA implementation as well as an analysis of the security issues related to APUF FPGA implementation. Lastly, almost all of the original paper has been rewritten with more text and additional figures to clearly explain the theory behind the IPUF design. The source code for this paper is publicly available at Github: Defense Attack (DA) PUF Library.

[1]Where an attacker only has access to challenge-response pairs. Once a silicon PUF design can be argued to be secure in this setting with respect to state-of-the-art machine learning (ML) attacks, it becomes an open problem to improve its implementation to resist side-channel attacks as well.

space of Challenge-Response Pairs (CRPs) which is impractical to enumerate[2] – making the PUF '*strong*'.

Lightweight Design. In a lightweight silicon PUF design manufacturing variations are exploited by *analogue computing* (e.g., two stimuli racing against one another through a multiplexer circuit in an Arbiter PUF [GCvDD02] as described in Fig. 4 in Appendix 9.1). After the analogue computing, an *analogue to digital conversion* takes place (e.g., by using an arbiter gate in an APUF). Next, in order keep the design lightweight two factors must be considered. First, the implementation must have a small number of gates (small area). Second, only *limited digital computation* is allowed with only a small number of gate computations and without the need for accessing additional memory. This gives a small hardware footprint and high throughput.

Strong lightweight silicon PUF designs that build on top of the APUF are the XOR APUF [SD07], the Feed-Forward PUF [LLG+05], LSPUF [MKP08], and Bistable Ring PUF [CCL+11]. Other examples of strong silicon PUF designs are the Power Grid PUF [HAP09], Clock PUF [YKL+13] and Crossbar PUF [RJB+11]. Since these other examples are either not lightweight or lack precise security arguments with respect to an extensive study of possible attack methodologies, we focus in this paper on designs that build on top of APUFs.

Security Argument. We consider an adversarial model in which an attacker attempts to obtain a software model of a PUF by using information extracted from measured CRPs. Intrinsically, a PUF hides a "random" function and learning such functions from input-output pairs is the field of ML – therefore, security must be argued with respect to the best known applicable ML techniques:

Classical ML Attacks. In this paper we refer to ML attacks that use non-repeated measurements of CRPs as *Classical* Machine Learning (CML): This type of attack was first introduced in 2004, where the 64 bit APUF was shown to be vulnerable with respect to SVM [Lim04, LLG+05]. As a proposed secure alternative, the 64-bit x-XOR APUF [SD07] xors the outputs of x APUFs into one response (see Fig. 5 in Appendix 9.1). However, Ruhrmaier et al. [RSS+10] demonstrated how the x-XOR APUF for $x \leq 5$ can be modeled with at least 98% accuracy using Logistic Regression (LR) with non-repeated measurements of CRPs. Probably Approximately Correct (PAC) learning has shown to be successful against the x-XOR APUF for $x \leq 4$ [GTS15, GTS16], while the state-of-the-art implementation of LR breaks the 64 bit x-XOR APUF up to $x \leq 9$ and a 128 bit x-XOR APUF up to $x \leq 7$ [TB15]. For larger x the XOR APUF has been shown to resist LR due to the subexponential relationship between x and the amount of training data required to model the XOR APUF [RSS+10, TB15].

The Bistable Ring PUF borrows from the APUF design and can be broken like the APUF using a neural network [SH14] or SVM [XRHB15]. The Feed-Forward APUF (FFA) [LLG+05] is another variant of the APUF and can be broken using SVM, LR and CRP based CMA-ES for ≤ 8 feedforward positions [RSS+10]. For a larger number of feedforward positions the FFA becomes unreliable and is therefore not considered to be practical.

The Lightweight Secure PUF (LSPUF) [MKP08] is a variant of the XOR APUF with multiple outputs. The LSPUF is based on the x-XOR PUF and consequently is vulnerable to LR [SNMC15] when $x \leq 9$.

Reliability Based ML Attacks. Becker [Bec15] was able to break the XOR APUF (and as a consequence the LSPUF) with a linear complexity in x using a non-classical ML attack which uses the reliability information of CRPs. Reliability information can be extracted from repeated measurements of responses belonging to the same challenge [DV13]. This

[2] Assuming no additional physical limitation on the read-out speed of CRPs from the PUF.

allows an attacker to measure the sensitivity of a response to environmental noise caused by e.g. temperature and voltage variations. In this paper we refer to attacks that use repeated CRP measurements as *Reliability based* Machine Learning (RML).[3]

Note that if responses are not sensitive to environmental noise, i.e., the PUF is very reliable, then Becker's reliability based CMA-ES attack is not applicable. For this reason one may want to add digital circuitry to the PUF in the form of a fuzzy extractor [DRS04] or an interface that exploits the LPN problem [JHR+17], but these techniques are not lightweight and therefore do not solve the stated fundamental problem. A more lightweight solution is presented in [WGM+17] where the reliability of an x-XOR APUF is enhanced using majority voting. However, this is not sufficiently lightweight as the same circuitry (including memory for storing a counter) needs to be executed repeatedly a large number of times which implies a large number of gate computations and reduction in throughput. But more important, majority voting does *not prevent* the reliability based CMA-ES attack as the environment can be pushed to extremes in order to make the PUF more unreliable again. We introduce the Interpose PUF (IPUF) which resists all state-of-the-art classical and reliability based ML attacks and, in particular, *prevents* the reliability based CMA-ES attack.

ML Categorization. In addition to partitioning ML attacks into classical and reliability based types, we can further categorize ML into *black box* (B) and *white box* (W) attacks. White box attacks can be further divided into two subcategories, derivative Free (FW) attacks and Derivative based (DW) attacks. Black box attacks are weaker than white box attacks in terms of modeling efficiency because they do not use an exact mathematical model of the PUF. Derivative Free (FW) attacks are less efficient compared to Derivative based (DW) attacks because they do not use derivative information for optimization. We express this relationship in

$$\text{B attacks} < \text{FW attacks} < \text{DW attacks}. \tag{1}$$

We summarize the state-of-the-art results in Table 1. Due to the existence of reliability ML attacks [Bec15], the fundamental problem of designing a secure, reliable, and lightweight strong silicon PUF becomes even more challenging.

Contributions, Storyline, and Organization.

1. Contribution - Reliability based ML Analysis. We provide a brief description of the APUF and the XOR APUF in Appendix 9.1. In Section 2 we cover the basic delay based and reliability based APUF models. In Section 2 we also go over the design of the (x, y)-IPUF (see Fig. 1). In Section 3 we describe the attacks that are relevant to the IPUF: Becker's reliability based (CMA-ES) ML attack on APUFs and XOR APUFs (i.e., RFW), as well as how the IPUF can be linearly approximated as an XOR APUF model in order to later analyze into what extend the classical and reliability based ML attacks on the XOR APUF apply to the IPUF.

After this background we comprehensively analyze the working of Becker's attack in Section 4. Through theoretical study and rigorous simulation and experimentation we explain why the attack works on APUFs and XOR APUFs and under what circumstances the attack fails. Based on this analysis, we improve (detailed in Appendices 9.8 and 9.9) Becker's attack.

2. Contribution - IPUF Design and Analysis. Based on our analysis of enhanced reliability based ML and our understanding about when this fails, we are now able to argue the security of the new IPUF design in Section 5:

[3]Reliability information can be regarded as a type of 'side-channel' information which is extracted from CRPs alone without the use of extraneous equipment, whereas additional equipement is needed in power side-channel analysis etc. [RXS+14, TDF+14, TLG+15]. In this paper security is argued in an adversarial model where the attacker only has access to CRPs.

Table 1: Vulnerability of different PUF designs to machine learning attacks.

		PUF Design		
		APUF	x-XOR APUF	(x,y)-IPUF
Attacks	CB	Insecure [RSS+10, GTFS16]	Secure	Secure
	CFW	Insecure [RSS+10, GTS15]	Secure	Secure
	CDW	Insecure [RSS+10]	Secure	Prevented
	RFW	Insecure [Bec15]	Insecure [Bec15]	Prevented
	RDW	Insecure [DV13]	N/A	N/A

CB = **Classical Black** box attacks (PAC [GTFS16], Neural Networks [RSS+10])
CFW = **Classical** derivative **Free White** box attacks (CRP based CMA-ES [RSS+10])
CDW = **Classical Derivative** based **White** box attacks (PAC [GTS15], SVM and LR [RSS+10])
RFW = **Reliability** derivative **Free White** box attacks (reliability based CMA-ES [Bec15])
RDW = **Reliability Derivative** based **White** box attacks (reliability based Least Squares [DV13])
N/A = Not Applicable and note that there are no known reliability based black box attacks

We will mention in Section 3 that the known reliability derivative based white box attack (RDW) cannot be used against the XOR APUF and by extension the IPUF. We show that *direct* application of Becker's attack is not applicable to the IPUF. Therefore, the way to attack an IPUF is through (a) an *indirect* application of a reliability derivative free white box attack (RFW) by approximating the IPUF as an XOR APUF, or (b) through classical ML attacks (CB, CFW, or CDW). We prove that classical derivative based white box ML (CDW) reduces to attacks that first approximate the IPUF as an XOR APUF and then apply classical ML on the approximated XOR APUF (this is detailed in Appendix 9.4). We further show that, through careful choice of the IPUF design parameters (x, y, and the 'interpose' position), approximating the IPUF by an XOR APUF introduces modeling inaccuracies and corresponding RFW and CDW attacks using this approximation can be *prevented*. We explain that classical black box attacks (CB) are not feasible against the IPUF (see Appendix 9.6). This leaves only classical white box ML that is derivative free (CFW), i.e. CRP based CMA-ES. We experimentally and analytically show that the complexity of CFW attacks on a $(y + x/2)$-XOR APUF is equivalent to the complexity of CFW attacks on a (x, y)-IPUF (as shown in Appendix 9.3). Hence, when x and y are properly chosen (just like choosing a high x in an XOR APUF) the IPUF is secure against CFW as well. We conclude that the *IPUF design solves the fundamental problem* of strong silicon PUFs with respect to all state-of-the-art ML attacks.

Finally, note that under state-of-the-art classical ML, the x-XOR APUF must resists both CFW and CDW attacks, the latter requires $x \geq 8$ for 128 bit challenges. Under state-of-the-art classical ML, the IPUF only needs to resist the CFW attack (since known CDW attacks can be prevented). The equivalence proof shows that this means that $y + x/2$ must be chosen large enough for an $(y + x/2)$-XOR APUF to resist CFW. In this case, see Ineq. (1), $y + x/2$ can be chosen smaller than 8 (because we do not need to resist CDW). Therefore, under classical ML with respect to CFW the $(1, 4)$-IPUF is the best choice (given simulations in Section 6 using CRP based CMA-ES). This implies a smaller number of APUFs compared to a 8-XOR APUF, making the IPUF more reliable and lightweight as compared to the XOR APUF. For all of these reasons, the *IPUF supersedes the XOR APUF as a strong PUF primitive.*

Sections 6 and 7 (with Appendices 9.7, 9.10 and 9.11) confirm our results and model by simulations and experiments with an IPUF FPGA implementation.

3. Contribution - Open Source PUF Library. We provide open source code for all of our simulations and experiments. This includes code for ML attacks on APUFs, XOR APUFs and IPUFs in Matlab and C#. Code to create various PUF models on FPGA hardware is also given.

We offer concluding remarks in Section 8.

2 The APUF and Interpose PUF

In this section, we briefly introduce the analytical delay model [Lim04] and reliability model [DV13] of the APUF. We also discuss the basic design of the newly proposed (x, y)-IPUF. Descriptions of both designs are necessary to understand the effectiveness of ML attacks on PUFs in Section 3. The reader can find the detailed description of the APUF and the XOR APUF in Appendix 9.1.

2.1 The APUF Linear Additive Delay Model

In [Lim04, LLG+05], an analytical model called the *Linear Additive Delay Model* was presented. As shown in [Lim04], the linear additive delay model of an APUF has the form:

$$\Delta = \mathbf{w}[0]\mathbf{\Phi}[0] + \cdots + \mathbf{w}[i]\mathbf{\Phi}[i] + \cdots + \mathbf{w}[n]\mathbf{\Phi}[n] = \langle \mathbf{w}, \mathbf{\Phi} \rangle, \tag{2}$$

where $\mathbf{w}$ and $\mathbf{\Phi}$ are known as *weight and parity (or feature) vectors*, respectively. The parity vector $\mathbf{\Phi}$ is derived from the challenge $\mathbf{c}$ as follows:

$$\mathbf{\Phi}[n] = 1, \quad \text{and} \quad \mathbf{\Phi}[i] = \prod_{j=i}^{n-1}(1 - 2\mathbf{c}[j]), i = 0, \ldots, n-1. \tag{3}$$

In this delay model, the unknown weight vector $\mathbf{w}$ depends on the process variation of the APUF instance (i.e. of a specifically manufactured APUF). The response to a challenge $\mathbf{c}$ is defined as: $r = 0$ if $\Delta \geq 0$. Otherwise, $r = 1$.

2.2 The APUF Reliability Model

Due to noise, the reproducibility or reliability of the output of the PUF is not perfect, i.e., applying the same challenge to a PUF will not produce a response bit with the same value every time. The repeatability is the *short-term reliability of a PUF* in presence of CMOS noise, and it is not the long-term device ageing effect [DV13].

In an APUF we can measure the (short-term) reliability R (i.e., repeatability) for a specific challenge $\mathbf{c}$ in the following way: Assume that the challenge $\mathbf{c}$ is evaluated M times, and suppose the measured responses that are equal to 1 is N out of M evaluations. The reliability is defined as $R = N/M \in [0, 1]$.

In Eq. (2) we showed the mathematical relationship between the parity vector $\mathbf{\Phi}$ and the corresponding response Δ. Similarly, there exists a mathematical relationship between the reliability R of a given challenge and its response Δ as shown in [DV13]:

$$\Delta/\sigma_N = \sum_{i=0}^{n}(\mathbf{w}[i]/\sigma_N)\mathbf{\Phi}[i] = -\Phi^{-1}(R) \tag{4}$$

where the noise follows a normal distribution $\mathcal{N}(0, \sigma_N)$ and $\Phi(\cdot)$ is the cumulative distribution function of the standard normal distribution. In the case where $R \in [0.1, 0.9]$ a further approximation [DV13] can be made:

$$\Delta/\sigma_N \approx R. \tag{5}$$

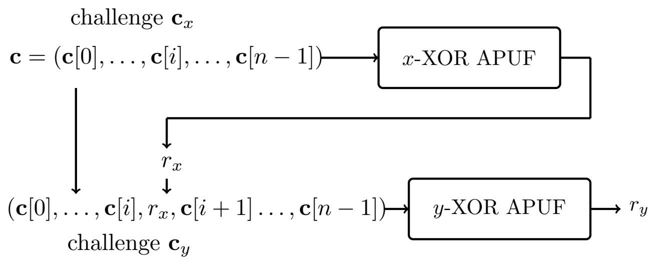
challenge $\mathbf{c}_x$
$\mathbf{c} = (\mathbf{c}[0], \ldots, \mathbf{c}[i], \ldots, \mathbf{c}[n-1])$
x-XOR APUF
r_x
$(\mathbf{c}[0], \ldots, \mathbf{c}[i], r_x, \mathbf{c}[i+1] \ldots, \mathbf{c}[n-1])$
y-XOR APUF
r_y
challenge $\mathbf{c}_y$

Figure 1: The (x, y)-IPUF (Interpose PUF) is comprised of an x-XOR APUF whose input r_x is interposed between $c[i]$ and $c[i+1]$ in the input of a y-XOR APUF.

2.3 The IPUF Design

A (x, y)-IPUF consists of two layers. The upper layer is an n-bit x-XOR APUF and the lower layer is an $(n+1)$-bit y-XOR APUF. We denote the input to the x-XOR APUF as $\mathbf{c}_x = (\mathbf{c}[0], \ldots, \mathbf{c}[i], \mathbf{c}[i+1], \ldots, \mathbf{c}[n-1])$. The response r_x of the x-XOR APUF is interposed in $\mathbf{c}_x$ to create a new $n+1$ bit challenge $\mathbf{c}_y = (\mathbf{c}[0], \ldots, \mathbf{c}[i], r_x, \mathbf{c}[i+1], \ldots, \mathbf{c}[n-1])$. The final response bit is the response r_y of the y-XOR APUF with respect to the new challenge $\mathbf{c}_y$. The structure of the (x, y)-IPUF is shown in Fig. 1.

When creating an (x, y)-IPUF three important parameters determine its security against ML attacks. The three parameters are x which represents the number of APUFs in the upper layer XOR APUF, y which represents the number of APUFs in the lower layer XOR APUF, and the place where the response of the upper layer r_x is interposed in the input challenge for the lower layer y-XOR APUF. In the next two sections we go over more details related to the ML attacks on PUFs including the (x, y)-IPUF. Based on this knowledge, we explain how to properly choose the security parameters for the (x, y)-IPUF in Section 5.3 to secure it against various ML attacks.

3 Reliability Based ML Attacks

Conceptually, instead of using CRPs like in Classical ML (CML) attacks, the *repeatability* (i.e. short-term reliability) of APUF outputs can be used to build an APUF model based on a set of challenge-reliability (not response) pairs. The relationship between reliability, R and the weights $\mathbf{w}$ of an APUF were shown in Eq. (4) and Eq. (5). In [DV13] a Reliability based ML (RML) attack was done under the assumption that $R \in [0.1, 0.9]$. Based on this assumption a system of linear equations was established using Eq. (5) so that $\mathbf{w}[i]/\sigma_N$ could be solved for by using the *Least Mean Square* algorithm. This approach only applies to the APUF, and not the XOR APUF and by extension it also does not apply to the IPUF (i.e. RDW is not applicable). However, RML attacks can be done **without** assumptions about the range of R, as we will explain in Section 3.1

In Section 3.2 we show how to model the IPUF as a linear approximation (LA) of an XOR APUF. This can be used to analyze into what extend the CML and RML attacks on the XOR APUF apply to the IPUF.

3.1 Reliability Based CMA-ES

In [Bec14, Bec15] a ML attack on APUFs was developed using CMA-ES with reliability information obtained from the repeated measurements of CRPs. More precisely, the reliability information R of a challenge $\mathbf{c}$ (i.e. $(\mathbf{c}, R)$) is used in the attack instead of the corresponding response r (i.e. $(\mathbf{c}, r)$).

The rationale behind this attack is as follows: if the delay difference $|\Delta|$ between the two competing paths in an APUF for a given challenge $\mathbf{c}$ is smaller than a threshold ϵ, then the corresponding response r would be unreliable in the presence of noise; otherwise the response would be reliable. This implies that reliability information directly leaks information about the "wire delays" in an APUF model. Let r_i be the i-th measured response of challenge $\mathbf{c}$ for $i = 1, \ldots, M$. Two different definitions of R, as provided in Eq. (6) and Eq. (7), are found in [DV13] and [Bec15], respectively:

$$R = \frac{1}{M}\sum_{i=1}^{M} r_i, \tag{6}$$

$$R = |M/2 - \sum_{i=1}^{M} r_i|. \tag{7}$$

Note similar to Eq. (6) and Eq. (7), repeatability for an APUF was defined as $R = N/M \in [0,1]$ (see Section 2.2). The objective of CMA-ES is to learn weights $\mathbf{w} = (\mathbf{w}[0], \ldots, \mathbf{w}[n])$ together with a threshold value ϵ. All variables $\mathbf{w}[0], \ldots, \mathbf{w}[n]$ are treated as independent and identically distributed Gaussian random variables. The attack is conducted as follows:

1. Collect N challenge-reliability pairs

$$\mathcal{Q} = \{(\mathbf{c}_1, R_1), \ldots, (\mathbf{c}_i, R_i), \ldots, (\mathbf{c}_N, R_N)\}.$$

2. Generate K random models:

$$\{(\mathbf{w}_1, \epsilon_1), \ldots, (\mathbf{w}_j, \epsilon_j), \ldots, (\mathbf{w}_K, \epsilon_K)\}.$$

3. For each model $(\mathbf{w}_j, \epsilon_j)$ $(j = 1, \ldots, K)$, do the following steps:

   (a) For each challenge $\mathbf{c}_i$ $(i = 0, \ldots, N)$, compute the R'_i as follows:

   $$R'_i = \begin{cases} 1, & \text{if } |\Delta| \geq \epsilon \\ 0, & \text{if } |\Delta| < \epsilon, \end{cases} \tag{8}$$

   where $\epsilon = \epsilon_j$ and Δ follows from (2) and (3) with $\mathbf{c} = \mathbf{c}_i$ and $\mathbf{w} = \mathbf{w}_j$. Note that for a given model $\mathbf{w}_j$ with input $\mathbf{c}_i$, R'_i indicates whether the output of the response of the model is reliable or noisy.

   (b) Compute the Pearson correlation coefficient ρ_j based on $(R_1, \ldots, R_i, \ldots, R_N)$ and $(R'_1, \ldots, R'_i, \ldots, R'_N)$.

4. CMA-ES keeps L models $(\mathbf{w}_j, \epsilon_j)$ which have the highest Pearson correlation ρ, and then, from these L models, another K models are generated based on the CMA-ES algorithm.

5. Repeat steps (3)-(4) for T iterations and model $(\mathbf{w}, \epsilon)$ which has highest Pearson correlation ρ will be chosen as the desired model. Note that sometimes the chosen model may have low prediction accuracy and in this case we restart the algorithm to find a model with higher prediction accuracy.

While the above pseudo-code is used to model an APUF, it can also be used to model an x-XOR APUF. Let

$$\mathcal{Q} = \{(\mathbf{c}_1, R_1), \ldots, (\mathbf{c}_i, R_i), \ldots, (\mathbf{c}_N, R_N)\}$$

Table 2: Relationship between the APUF model converged to by CMA-ES and the APUF's data set noise rate proportion in each data set $\mathcal{Q}$

Rank	$n=1$	$n=2$	$n=3$	$n=4$	$n=5$	$n=6$	$n=7$	$n=8$	$n=9$	$n=10$	Failed
Occurrence	36%	5%	9%	5%	12%	7%	7%	5%	7%	5%	2%

Rank: APUF model had the n-th highest data set noise proportion in the data set.
Failed: Failed to converge to any APUF model.
Occurrence: Percentage of time a convergence occurred.

be a set of challenge-reliability pairs of an x-XOR APUF instance. If the CMA-ES algorithm for modeling an APUF is executed many times with the set $\mathcal{Q}$, then it can produce x different models for $A_0, \ldots, A_{x-1}$ with high probability [Bec15]. Although there is no proof on how many times the CMA-ES algorithm has to be executed to get the models of all APUF instances of the x-XOR APUF, experimentally it is observed that this value needs not to be large. As done in [Bec15], one can parallelize CMA-ES executions to build models for $A_0, \ldots, A_{x-1}$.

As explained above, the modeling of an x-XOR APUF simplifies to the modeling of x independent APUF instances in the reliability based CMA-ES attack. This is significant because the relationship between x and the number of CRPs needed for the reliability based CMA-ES attack is linear. As previously stated, CML attacks have an exponential relationship between the number of CRPs and x. Therefore increasing x is a valid way to mitigate the CML attack. However, the reliability based CMA-ES attack cannot be defeated in the same manner.

In Appendices 9.8 and 9.9, we describe enhancements to the original reliability based CMA-ES attack [Bec15] allowing smaller training sets for achieving the same accuracy in our simulations and experiments.

3.2 Linear Approximation of the (x, y)-IPUF

A technique that can be used in conjunction with CML or RML is linear approximation; this technique is specifically designed for use against the (x, y)-IPUF. We develop the technique based on the following observation: The difference between the input challenge to the y-XOR APUF in an (x, y)-IPUF and the input to a standard y-XOR APUF is only one bit. Assume $i + 1$ is the interposed bit position for the input challenge to the y-XOR APUF in an (x, y)-IPUF. The input to the y-XOR APUF is denoted as $\mathbf{c}_{low} = (\mathbf{c}[0], \ldots, \mathbf{c}[i], r_x, \mathbf{c}[i+1], \ldots, \mathbf{c}[n-1])$. Instead of attempting to learn the x-XOR APUF in the (x, y)-IPUF to estimate r_x, we can give a fixed value for bit $i + 1$, i.e. $\mathbf{c}'_{low} = (\mathbf{c}[0], \ldots, \mathbf{c}[i], 0, \mathbf{c}[i+1], \ldots, \mathbf{c}[n-1])$.

By making this approximation we can effectively ignore the x-XOR APUF component of the (x, y)-IPUF and treat the (x, y)-IPUF as a y-XOR APUF. Through this approximation we can do both CML and RML attacks on the (x, y)-IPUF while still using the XOR APUF model. These attacks are denoted as LA-CML and LA-RML. In Section 5.2.2 we analyze under what conditions the linear approximation accurately approximates the (x, y)-IPUF and how this attack can be mitigated.

4 Analysis of the Reliability based CMA-ES Attack

The reliability based CMA-ES attack is a serious security issue when designing a PUF. Our goal is to create a secure PUF design (the (x, y)-IPUF) that *prevents* this attack. To do this, it is necessary to understand under what conditions the reliability based CMA-ES attack works. In this section, we consider the following questions for in-depth analysis of the reliability based CMA-ES attack:

1. In [Bec15] it is noted that CMA-ES converges more often to some APUF instances than others when modeling the components of an x-XOR APUF. Essentially this means some APUFs in an x-XOR APUF are *easier* and some are *harder* to model using the given challenge-reliability pairs. Why does this happen?

2. What are the conditions such that CMA-ES never converges to a particular APUF instance? In other words, under which condition does the reliability based CMA-ES attack fail?

The first question was posed in [Bec15] without any theoretical answer and the second question has not been investigated in literature. The next experiments are aimed at answering these questions. Based on the knowledge gained from these experiments, we develop the (x, y)-IPUF that is secure against the reliability based CMA-ES attack as well as the other machine learning attacks mentioned in Section 3.

4.1 Experiment-I: Understanding CMA-ES Convergence

The objective of this experiment is to analyze why some APUF instances are *easier* and some are *harder* to model using reliability based CMA-ES. More specifically, we want to verify whether the probability of converging to an APUF model in CMA-ES is correlated with the "data set noise proportion" of that APUF instance present in a given data set $\mathcal{Q}$. Here we define the data set noise proportion for a particular APUF in an x-XOR APUF as the number of noisy (unreliable) CRPs due to the specified APUF divided by the number of total CRPs in $\mathcal{Q}$.

Experimental Setup: We run the CMA-ES algorithm 100 times on a 10-XOR APUF. Each time we run CMA-ES we use a new randomly generated dataset $\mathcal{Q}$ which contains 70×10^3 CRPs. The noise rate of each individual APUF is 20%. It is important to note that while the noise rate of each APUF is the same, the data set noise proportion of each APUF in $\mathcal{Q}$ will change each time we generate a new $\mathcal{Q}$. For each $\mathcal{Q}$, we generate the challenge-reliability pair for $\mathcal{Q}$ by measuring the response to each challenge 11 times.

Experimental Results: The results of experiment I are summarized in Table 2. In each run of CMA-ES, a model $\mathbf{w}$ is generated. We classify the model in the following way: if the model $\mathbf{w}$ matches one of the APUF models with probability ≥ 0.9 or ≤ 0.1 (complement model), then we accept it as a *correct* model for that particular APUF instance. If the generated model $\mathbf{w}$ does not match any of the APUF models we consider the CMA-ES algorithm to have failed to correctly converge. Note that $\mathbf{w}$ can match with at most one APUF instance. This is because if the model $\mathbf{w}$ corresponds to a particular APUF instance, then only that instance will have a matching probability ≥ 0.9 or ≤ 0.1, and the other APUF instances will have a matching probability around 0.5. This is due to the good uniqueness property of simulated APUF instances.

For the given $\mathcal{Q}$, we measure the data set noise proportion of each APUF with respect to the challenges present in $\mathcal{Q}$. If CMA-ES converges to the APUF model with the highest data set noise proportion in the current $\mathcal{Q}$, we increment the count in column one. If CMA-ES converges to the APUF model with the second highest data set noise proportion in the current $\mathcal{Q}$, we increment the count in column two and so on. If the CMA-ES algorithm generates a model that corresponds to none of the APUFs then we say it failed to converge to any model.

Analysis of Results: The experimental results can be explained as follows. Every time we generate a new set $\mathcal{Q}$, the challenge-reliability pairs $\{(\mathbf{c}_i, R_i)\}$ of $\mathcal{Q}$ can be divided into two parts. The first part is made up of the reliable challenge reliability pairs $\mathcal{Q}_r$ and the second part is made up of the noisy challenge-reliability pairs $\mathcal{Q}_n$. Each APUF instance A_i has its own set of noisy challenge-reliability pairs $\mathcal{Q}_{i,n} \subset \mathcal{Q}_n, i = 0, \ldots, 9$. The

CMA-ES algorithm tries to converge to the APUF instance which has the largest number of pairs in the combined set $\mathcal{Q}_r \cup \mathcal{Q}_{i,n}$, i.e., highest Pearson correlation (see Step-4 of the reliability based CMA-ES attack in Section 3.1). Since $\mathcal{Q}_r$ is useful for modeling all the APUF instances, the set $\mathcal{Q}_{i,n}$ should be large to make the $\mathcal{Q}_r \cup \mathcal{Q}_{i,n}$ sufficient enough for modeling the i-th APUF instance. In other words, CMA-ES tries to converge to the APUF instance that has the largest value for $|\mathcal{Q}_{i,n}|/|\mathcal{Q}|$.

The PUF with the highest data set noise rate proportion in $\mathcal{Q}$ should have the highest Pearson correlation coefficient and therefore be the global maximum. However CMA-ES does not guarantee convergence to the global maximum. When CMA-ES converges to a local maximum, it produces another one of the valid APUF models, or an invalid model. For this reason we can see in Table 2 that we can converge to a PUF model that does not have the highest noise proportion with small probability compared to the highest case, i.e.,

$$\frac{5}{100}, \frac{7}{100}, \frac{9}{100}, \frac{12}{100} \ll \frac{36}{100}.$$

Overall every time we generate $\mathcal{Q}$, the PUF with the highest noise proportion in $\mathcal{Q}$ will have a high probability of being found by CMA-ES (i.e., 36/100). Likewise, the PUFs with a smaller noise proportion in $\mathcal{Q}$ will have a smaller probability of being found.

4.2 Experiment-II: CMA-ES Reliability Conditions

The objective of this experiment is to understand under which condition the reliability based CMA-ES attack fails to build a model for a particular APUF in an x-XOR APUF. From experiment I we know that CMA-ES is most likely to converge to the APUF model which has the highest data set noise proportion in $\mathcal{Q}$. We want to show that if the noise rate of the APUF instances in the x-XOR APUF's output are *not equal* (i.e., drawn from different distribution), then some APUF models cannot be generated by CMA-ES.
Experimental Setup: We simulate a 2-XOR APUF consisting of two APUF instances, denoted as A_0 and A_1. The noise rate of both APUFs are set at 1%. We run CMA-ES on the 2-XOR APUF 100 times. In each run of CMA-ES we generate a $\mathcal{Q}$ of size 70×10^3, where in $\mathcal{Q}$ each challenge is evaluated 11 times to generate the reliability information.

In this experiment we hypothesize that CMA-ES fails to build a certain APUF model when that model always has a lower noise rate (and therefore a lower data set noise proportion in $\mathcal{Q}$). To do this we manipulate the reliability information presented in the final output, such that A_0 always has lower data set noise proportion. This is achieved by applying majority voting to the responses of A_0 before XOR-ing it with the response of A_1. In majority voting, we have experimented with 5 and 10 votes to observe the performance of CMA-ES.

Experimental Results: The experimental results are shown in Table 3. The first column corresponds to the number of times the output was measured on A_0 before majority voting was done. The second and the third columns refer to the number of times the correct model was found by CMA-ES for A_0 and A_1, respectively.

Analysis of Results: From Table 3, it is clear that if M is sufficiently large ($M \geq 10$), then the reliability based CMA-ES attack cannot build a model for A_0. This is because we decreased the noise rate of A_0 by applying majority voting. Since A_0 is less noisy, it will have a lower data set noise proportion in $\mathcal{Q}$. As we established in the first experiment, CMA-ES tends to converge to the model with highest data set noise proportion with high probability. In Table 3 we can clearly see this happening when $M = 10$, as CMA-ES is never able to build a model for A_0 (the APUF with the lower data set noise proportion).

It is important to also note that just because the APUFs have different noise rates, it does not make the XOR APUF secure against the reliability based CMA-ES attack. In the setup described in this experiment, an attacker could simply learn a model for A_1.

Once the model for A_1 has been learned the attacker could then use that model to remove most of the noisy challenge-reliability pairs corresponding to A_1 from $\mathcal{Q}$. Doing this would create a new dataset $\mathcal{Q}_{reduced}$ from $\mathcal{Q}$ in which A_0 would have the highest data set noise proportion. The attacker could then run CMA-ES on $\mathcal{Q}_{reduced}$ to get a model for A_0.

Table 3: Results of Experiment-II

$M^{\dagger}$	Number of times A_0 found	Number of times A_1 found
5	8	92
10	0 ‡	99 ‡

† No. of measurements used in the majority voting of A_0.

‡ The sum of the two counts is not equal to 100 because one attack failed.

4.3 Inferences from the Experiments

Two important points can be understood from the experiments in this section. In order for the reliability based CMA-ES attack to be successful the following conditions must be met:

1. All APUF instances outputs must have the same influence on the final output of the PUF.
2. The noise rate of all APUF instances should be similar.

In the next section, we leverage the knowledge from these experiments to show how the proposed IPUF can be secured against the reliability based CMA-ES attack.

5 Security and Reliability Analysis of IPUF

In this section, we analyze the security and reliability of the proposed (x, y)-IPUF design. There are three main parameters to choose when designing an (x, y)-IPUF: x, y and the position of the interposed bit. By selecting the right parameter values, we show that our (x, y)-IPUF can be secured against all the aforementioned ML attacks enumerated in Table 1.

This section is organized as follows: To explain how to properly choose the (x, y)-IPUF parameters in Section 5.1 we first show how a single challenge bit in an APUF effects its output r. We then use this analysis to determine the most secure position for the interposed bit in a $(1, 1)$-IPUF in Section 5.2. Since the IPUF is developed to *prevent* RML attacks, we need to study the reliability of the $(1, 1)$-IPUF as shown in Section 5.2.1. After that, we explain why IPUF's design can *prevent* RML attacks. While the $(1, 1)$-IPUF can prevent RML attacks, properly choosing the interposed bit position alone is not enough. The $(1, 1)$-IPUF still suffers from CML, LA-CML and LA-RML attacks (see Section 3.2). Therefore, in Section 5.3 we expand our analysis to the (x, y)-IPUF where $x \geq 1$ and $y > 1$. By using a middle interposed bit and properly choosing x and $y \geq 2$ we are able to show that the (x, y)-IPUF is secure against all current state-of-the-art ML attacks. We comprehensively study the reliability of the IPUF in Appendix 9.7. Based on our analysis we claim properly designed IPUFs are superior to XOR APUFs in terms of security, reliability and hardware overhead.

5.1 Influence of Challenge Bit $\mathbf{c}[j]$ on the Response r in the APUF

The influence of a challenge bit on an APUF's response depends on its position in the challenge $\mathbf{c}$ [MKP09, DGSV14, NSCM16]. From Eq. (2), it can be observed that

$\mathbf{\Phi}[j+1],\ldots,\mathbf{\Phi}[n-1]$ does not depend on the challenge bit $\mathbf{c}[j]$. For a given challenge $\mathbf{c}$, based on the linear delay model of the APUF, the delay difference Δ can be described as:

$$\Delta = (1-2\mathbf{c}[j]) \times \Delta_{Flipping} + \Delta_{Non-Flipping} \tag{9}$$

where $\Delta_{Flipping}$ is the term affected by the flipping of bit $\mathbf{c}[j]$ and is given by $\Delta_{Flipping} = \sum_{i=0}^{j} \mathbf{w}[i]\frac{\mathbf{\Phi}[i]}{(1-2\mathbf{c}[j])}$. Likewise, the term that is not dependent on the flipping of $\mathbf{c}[j]$ is denoted as $\Delta_{Non-Flipping} = \sum_{i=j+1}^{n} \mathbf{w}[i]\mathbf{\Phi}[i]$.

If $\mathbf{c}[j]=0$ then $\Delta = \Delta_{Flipping} + \Delta_{Non-Flipping}$ and we will denote this Δ as $\Delta_{\mathbf{c}[j]=0}$ with corresponding response $r_{\mathbf{c}[j]=0}$. Similarly when $\mathbf{c}[j]=1$ we will have $\Delta = -\Delta_{Flipping} + \Delta_{Non-Flipping}$. We denote this Δ as $\Delta_{\mathbf{c}[j]=1}$ and the response as $r_{\mathbf{c}[j]=1}$.

We want to know the influence of flipping $\mathbf{c}[j]$ on the output r. We measure this influence by computing the probability that the output remains the same if we flip bit $\mathbf{c}[j]$ while keeping the rest of $\mathbf{c}$ constant:

$$\Pr_{\mathbf{c}}(r_{\mathbf{c}[j]=0} = r_{\mathbf{c}[j]=1}). \tag{10}$$

In Appendix 9.2, we prove:

$$\Pr_{\mathbf{c}}(r_{\mathbf{c}[j]=0} = r_{\mathbf{c}[j]=1}) \approx \frac{(n-j)}{n}, j = 0,\ldots,n-1 \tag{11}$$

This implies that an expected probability $\Pr_{\mathbf{c}}(r_{\mathbf{c}[j]=0} = r_{\mathbf{c}[j]=1})$ decreases with the increasing value of j, so the influence of each challenge bit is not equal. This undesirable security property means we must carefully consider the position of the interposed bit. In the next section we analyze how the interposed bit position effects the security and reliability of the $(1,1)$-IPUF.

5.2 Security and Reliability Analysis of the (1,1)-IPUF

The most basic form of the (x,y)-IPUF is the $(1,1)$-IPUF, with the upper layer consisting of a single APUF A_{up} and the lower layer consists of a single APUF A_{low}. Let us denote the responses to A_{up} and A_{low} by r_{up} and r_{low}, respectively. The final output of the $(1,1)$-IPUF is the response r_{low}. Based on the $(1,1)$-IPUF structure we analyze where to interpose the bit in the lower APUF and how this affects the reliability and security of the $(1,1)$-IPUF.

5.2.1 Reliability of the (1,1)-IPUF

In order to determine the effect of measurement noise in the $(1,1)$-IPUF, we evaluate a challenge $\mathbf{c}$ twice. Let us denote $r_{up,0}$ as the response of the upper APUF and $r_{low,0}$ as the response of the lower APUF the first time the challenge is applied. Likewise, let us denote $r_{up,1}$ and $r_{low,1}$ as the APUF's responses the second time the challenge is evaluated.

Assume APUF A_{up} has noise rate β_{up} such that $\Pr_{\mathbf{c}}(r_{up,0} \neq r_{up,1}) = \beta_{up}$. Similarly, assume that APUF A_{low} has noise rate β_{low} such that $\Pr_{\mathbf{c}}(r_{low,0} \neq r_{low,1} | r_{up,0} = r_{up,1}) = \beta_{low}$.

Let us denote $i+1$ as the interposed bit position for r_{up} in the $(n+1)$-bit challenge of A_{low}. We use Eq. (11) to derive

$$\begin{aligned}
& \Pr_{\mathbf{c}}(r_{low,0} \neq r_{low,1}) \\
= \; & \Pr_{\mathbf{c}}(r_{low,0} \neq r_{low,1} | r_{up,0} = r_{up,1}) \Pr_{\mathbf{c}}(r_{up,0} = r_{up,1}) + \\
& \Pr_{\mathbf{c}}(r_{low,0} \neq r_{low,1} | r_{up,0} \neq r_{up,1}) \Pr_{\mathbf{c}}(r_{up,0} \neq r_{up,1}) \\
= \; & \beta_{low}(1-\beta_{up}) + \left(\frac{i+1}{n+1}\right)\beta_{up}.
\end{aligned} \tag{12}$$

In practice $\beta_{up} \ll 1$ and $\beta_{low} \ll 1$, thus Eq. (12) can be approximated as:

$$\Pr_{\mathbf{c}}(r_{low,0} \neq r_{low,1}) \approx \beta_{low} + \beta_{up}\frac{i}{n} \tag{13}$$

From Eq. (12) and Eq. (13) it can be seen that the reliability information of A_{up} and A_{low} available at the output of $(1,1)$-IPUF are not *equal* even when $\beta_{low} = \beta_{up}$. If we assume $\beta_{low} = \beta_{up} = \beta$ then A_{low} contributes approximately β while A_{up} contributes approximately $\beta\frac{i}{n}$. The unequal reliability contribution shown by our analysis has important implications for the success of the reliability based CMA-ES attack.

5.2.2 Security of $(1,1)$-IPUF

We will now discuss the security of the (1,1)-IPUF with respect to the reliability based CMA-ES attack (i.e. RML), CML and ML attacks that use the linear approximation technique (i.e. LA-CML and LA-RML).

Reliability Based CMA-ES Attack: The (1,1)-IPUF is theoretically secure against the CMA-ES reliability attack for two reasons if the interposed bit position for r_{up} is properly chosen: The first reason is based on the conditions under which the CMA-ES attack operates and the second is based on the computation done to learn the APUF model in CMA-ES.

First, recall the conditions under which the reliability based CMA-ES attack works as described in Section 4.2. In order to successfully model the APUF components A_{up} and A_{low}, each APUF must contribute equal reliability information to the output. For the (1,1)-IPUF, we showed in Eq. (13) that the contributions of A_{low} and A_{up} are not equal, i.e., β is not equal to $\beta\frac{i}{n}$ when i is between 0 and $\frac{n}{2}$. Due to the unequal contribution of reliability information in the output when the interposed bit position $(i+1)$ is not close to n, CMA-ES will not converge to the model for A_{up}. We did the following experiment to determine the importance of the interposed bit position. We launched the reliability based CMA-ES attack on a 64-bit (1,1)-IPUF with 30,000 challenge-reliability pairs. In this experiment, the noise rate of each APUF was 20% ($\beta = 0.2$). The number of iterations for CMA-ES was 30,000. We repeated the attack 20 times with the interposed bit position at 0 ($i = 0$), i ($i = n/2$) and 64 ($i = n$). **The result shows that A_{up} can be modeled (i.e., the prediction accuracy of the model of A_{up} is 98%) when $i = n = 64$. However, if the inserted position is in the middle ($i = 32$) or at first stage ($i = 0$), then A_{up} can not be modeled (i.e., the prediction accuracy of the model of A_{up} is** 51%).

Since we cannot first build a model for A_{up} we must first try to build a model for A_{low}. This brings us to the second reason the (1,1)-IPUF is secure against the reliability based CMA-ES attack. Recall in Section 3.1 that Δ is needed to compute the fitness of each model $\mathbf{w}$. Δ is based on the input to A_{low}. However we do not know one of the input bits (the interposed bit) to A_{low} so we cannot compute Δ (see the calculation of Δ in Eqs. (2) and (3)).

However, we should take a closer look at the way the computation of Δ is done to know how the interposed bit position affects the modeling attack on A_{low}. In Section 5.1, we have $\Delta = (1 - 2\mathbf{c}[j]) \times \Delta_{Flipping} + \Delta_{Non-Flipping}$ (see Eq.(9)) and thus, if j gets closer to 0, then Δ and $\Delta_{Non-Flipping}$ become similar. Strictly speaking, we cannot run CMA-ES to build a model for A_{low} when the interposed bit position i is **NOT** close to 0, for example the interposed bit position is in the range of $[n/2, n]$.

Conclusion: We cannot model A_{up} due to the unequal reliability information on the output and we cannot model A_{low} due to the unknown value of the interposed bit when the interposed bit position is properly chosen. Therefore, we claim the $(1,1)$-IPUF is secure against the reliability based CMA-ES attack when the interposed bit position is properly chosen in the middle of the input to A_{low}.

Classical Machine Learning Attacks: The $(1,1)$-IPUF is not secure against classical machine learning attacks due to its low model complexity. Instead of modeling the APUF components individually, any machine learning algorithm can be used to learn the model for A_{low} and A_{up} simultaneously. Experiments to support our claim are given in Section 6 (see Table 4). Note that, while the IPUF is vulnerable to classical derivative free machine learning, we will prove that derivative based classical machine attacks are **not** possible on an IPUF in the next section. As a result, we only need to consider derivative free classical machine learning attacks on an IPUF.

Attacks Using Linear Approximation (LA-CML and LA-RML): The security of the $(1,1)$-IPUF against an ML attack that use the linear approximation (see Section 3.2) depends on the choice of the interposed bit position. In this attack, any CML or RML attack on an XOR PUF can be adapted to work on an (x,y)-IPUF. This adaptation is done by approximating the (x,y)-IPUF as a y-XOR APUF by fixing the interposed bit from the x-XOR APUF to be 0. In the case of the $(1,1)$-IPUF this means that we ignore the component A_{up} and approximate $(1,1)$-IPUF by APUF A_{low}.

Let us denote $\mathbf{c}_{low}$ as the input to A_{low} and $\mathbf{c}'_{low}$ to be the approximation of $\mathbf{c}_{low}$ where we fix the interposed bit r_{up} in $\mathbf{c}_{low}$ to be 0. We can write $A_{low}(\mathbf{c}'_{low})$ as the output of the linear approximation and $A_{low}(\mathbf{c}_{low})$ as the output of the $(1,1)$-IPUF. We can now analyze how effective the linear approximation is. We measure the effectiveness of the approximation by computing the probability that the output of the linearized model $A_{low}(\mathbf{c}'_{low})$ matches the output of $A_{low}(\mathbf{c}_{low})$:

$$p_{approx} = \Pr_{\mathbf{c}}(A_{low}(\mathbf{c}'_{low}) = A_{low}(\mathbf{c}_{low})) \tag{14}$$

If p_{approx} is high, then the $(1,1)$-IPUF **is accurately approximated** by APUF $A_{low}(\mathbf{c}'_{low})$ and can be modeled with an ML attack.

Let us assume the following conditions for the analysis of the attack and for the sake of explanation, we drop *low* from $\mathbf{c}'_{low}$ or $\mathbf{c}_{low}$. We model a $(x,1)$-IPUF with APUF components that are 100% reliable and the output r_{up} of the x-XOR APUF is uniform, i.e., $\Pr_{\mathbf{c}}(r_{up}=0) = \Pr_{\mathbf{c}}(r_{up}=1) = \frac{1}{2}$. Then,

$$\begin{aligned} p_{approx} &= \Pr_{\mathbf{c}}(A_{low}(\mathbf{c}') = A_{low}(\mathbf{c})) \\ &= \Pr_{\mathbf{c}}\left(A_{low}(\mathbf{c}') = A_{low}(\mathbf{c})|r_{up}=0\right)\Pr_{\mathbf{c}}(r_{up}=0) \\ &\quad +\Pr_{\mathbf{c}}(A_{low}(\mathbf{c}') = A_{low}(\mathbf{c})|r_{up}=1)\Pr_{\mathbf{c}}(r_{up}=1) \\ &= 1 \times 1/2 + \frac{n-i}{n} \times 1/2 = 1/2 + \frac{n-i}{2n}. \end{aligned} \tag{15}$$

Eq. (15) shows that p_{approx} decreases as i increases. **Note that our discussion holds for any $(x,1)$-IPUF and thus, it is applicable to the $(1,1)$-IPUF**. We model a 64-bit (1,1)-IPUF using the reliability based CMA-ES attack with the linear approximation (LA-RML). The number of challenge-reliability pairs was 30,000 and the noise rate was 20%. From the experiment, the prediction accuracy of LA-RML on a 64-bit (1,1)-IPUF when $i = 0, 32, 64$ is equal to $97\%, 70\%$ and 51%, respectively. Likewise, a similar result can be achieved by using CRP based CMA-ES (classical machine learning).

A prediction accuracy of 50% is the worst a machine learning attack can do on a PUF with uniform binary output. Therefore, it would seem that picking the interposed bit positon to be as high as possible would result in the most secure (x,y)-IPUF design. However, below we will explain why choosing a high interposed position is not ideal.

Interposed Bit Position: In the $(1,1)$-IPUF the only design parameter we must choose is the interposed bit position. The higher the interposed bit position, the more influence A_{up} has on the $(1,1)$-IPUF. As a result the PUF model is more complex. It is more difficult to attack with CML attacks and the linear approximation is less accurate. However, a high bit position yields high noise on the output (less reliable). In addition, with a high interposed bit position and large enough number of input bits, the $(1,1)$-IPUF becomes equivalent to an XOR APUF in terms of susceptibility to RML attacks.

The conclusion from the analysis of the $(1,1)$-IPUF is that using the interposed bit position as the only security parameter is not enough to mitigate all the different ML attacks. We seek a tradeoff between all the factors by choosing the interposed bit to be the middle bit position. Based on this choice we then analyze how to modify x and y to further secure our design in Section 5.3.

5.3 Security and Reliability Analysis of the (x, y)-IPUF

The analysis in Section 5.2.2 showed that the $(1,1)$-IPUF with a middle interposed bit position could defeat the reliability based CMA-ES attack. However the $(1,1)$-IPUF was still vulnerable to CML attacks and both types of attacks that employ the linear approximation (LA-CML and LA-RML). In this section, we show how selecting x and y can mitigate the remaining ML attacks and we prove that the derivative based classical machine learning attacks (CDW and see Table 1 for the classification of ML attacks) are not available. We also analyze other important properties of the (x,y)-IPUF including reliability (Appendix 9.7), the strict avalanche property (SAC) (Appendix 9.5) and the resistance of IPUF against PAC learning attacks (Appendix 9.6).

5.3.1 Security Analysis

In this section we show how the (x,y)-IPUF can mitigate the reliability based CMA-ES attack (RML), CML attacks, LA-CML and LA-RML.

Reliability based CMA-ES Attack: The security argument for the $(1,1)$-IPUF in Section 5.2.2 also applies to the (x,y)-IPUF. Using challenge-reliability pairs and CMA-ES, an adversary cannot build models for the x component APUFs in the x-XOR APUF. This is due to the unequal contribution of noise on the output between the x-XOR APUFs and the y-XOR APUFs (see Section 9.7). Also an adversary cannot build models for the y component APUFs in the y-XOR APUF as r_x (the interposed bit position) is not known. Therefore, we consider the (x,y)-IPUF to be secure against the reliability based CMA-ES attack.

Classical Machine Learning Attacks: There is no known way the APUF components of the (x,y)-IPUF can be modeled individually. As a result, the only way to attack an (x,y)-IPUF is by modeling all the $(x+y)$ component APUFs simultaneously using classical machine learning, e.g., neural network or CRP based CMA-ES. Ruhrmair *et al.* [RSS$^+$10] showed that the more APUFs that influence (contribute) to the output of an XOR APUF, the more difficult the PUF is to model using CML methods. In other words, increasing x in an x-XOR APUF can mitigate CML attacks. In Appendix 9.3, we prove that if the interpose position of r_x is i then the (x,y)-IPUF is equivalent to a $(y + p_r x)$-XOR APUF where:

$$p_r = \frac{1-(1-2p)^y}{2} \qquad \text{and} \qquad p = \frac{i}{n}.$$

If $i = n$ and y is odd, then $p_r = 1$ and (x,y)-IPUF is equivalent to $(x+y)$-XOR APUF in terms of security because of $(x+y)$ APUFs contributing to every challenge-response pair. If $i = 0$, then $p_r = 0$ and (x,y)-IPUF is equivalent to a y-XOR PUF. In terms of difficulty of modeling with classical machine learning methods (i.e. CRP based CMA-ES), the (x,y)-IPUF with parameter i is approximately equivalent to a $(y + p_r x)$-XOR PUF. We experimentally verify this claim in Section 6.1 (see Figs. 2 and 3). As a result, we can use the same strategy employed in XOR APUF design [RSS$^+$10] and increase x and y in an (x, y)-IPUF to mitigate classical machine learning attacks. It is also worth noting this analysis to determine the number of APUFs that contribute in an IPUF can be used to derive further IPUF properties such as uniformity, uniqueness and reliability.

LA-RML. Reliability based CMA-ES applied to an (x, y)-IPUF after linearly approximating it as a y-XOR APUF learns one single component APUF of the y-XOR APUF. In the linear approximation we substitute r_x from the upper x-XOR APUF by 0 and feed 0 into the lower y-XOR APUF. If we denote the single component APUF which we try to learn using CMA-ES by A_{low}, then, for the challenge interposed with r_x, the output of A_{low} is the output of an $(x, 1)$-IPUF. I.e., we attempt to learn a model for A_{low} from a linear approximation of an $(x, 1)$-IPUF. From Eq.(15) with interpose bit position in the middle we infer that the model at best predicts A_{low} with $p_{approx} = 75\%$ accuracy. Reliability based CMA-ES learns models for each of the component APUFs of the lower y-XOR APUF, each with at most 75% accuracy. This shows that the maximum accuracy of the learned approximated y-XOR APUF is at most

$$\begin{aligned} p^{XOR}_{learn} &= \sum_{j=0, j \text{ is even}}^{y} \binom{y}{j} (1 - p_{approx})^j p_{approx}^{y-j} \\ &= \frac{1 - (2p_{approx} - 1)^y}{2} = \frac{1}{2} + \frac{1}{2^{y+1}}. \end{aligned}$$

This shows that p^{XOR}_{learn} is close to 1/2 for y large enough and this implies that the learned model for the linearly approximated y-XOR APUF does not contain predictive value[4].

If $y \geq 3$, then $p^{XOR}_{learn} \leq 56.25\%$. We launched the LA-RML attack on a 64-bit (3,3)-IPUF. In this experiment the noise rate for each APUF was 20%. The prediction accuracy of the final model was around 50% (confirming the theoretical upper bound) when 200,000 challenge-reliability pairs were used in the training phase (see Table 4).

LA-CML. In case of linearly approximating the (x, y)-IPUF as a y-XOR APUF and applying classical ML, we know that learning a model for even a noise-free 64 bit y-XOR APUF is currently not practical for $y \geq 10$ if LR is used and not practical for even smaller y if CRP based CMA-ES is used. However, even if the IPUF itself is 100% reliable, a *reliable* CRP of the IPUF may be a *noisy* CRP of the linearly approximated y-XOR APUF. By combining Eq.(11) with the derivation leading to Eq.(15), the accuracy p^{XOR}_{approx} of the linearly approximated y-XOR APUF itself is given by

$$p^{XOR}_{approx} = 1 \times 1/2 + p' \times 1/2,$$

where

$$p' = \sum_{j=0, j \text{ is even}}^{y} \binom{y}{j} \left(\frac{i}{n}\right)^j \left(\frac{n-i}{n}\right)^{y-j} = \frac{1 + (1 - \frac{2i}{n})^y}{2}.$$

After substituting p' we obtain

$$p^{XOR}_{approx} = \frac{3}{4} + \frac{1}{4}(1 - \frac{2i}{n})^y.$$

If the interposed bit is at the middle position (i.e. $i = \frac{n}{2}$), then p^{XOR}_{approx} is 75%. This implies that the noise rate of the linearly approximated y-XOR APUF given by the CRPs from the IPUF is 25%. For this reason CML should be even more difficult: We performed

[4]We can compare the model's output with the IPUF's output and attempt to find out whether this teaches something about r_x. Due to the XOR in the lower y-XOR APUF, the outputs of individual component APUFs are masked so that little can be learned about r_x. For small $y = 1$, we are able to learn some information about r_x from comparing the model's output with the IPUF's actual output; this can then be used to learn about the upper x-XOR APUF.

the LA-CML attack using CRP based CMA-ES on a **reliable** 64-bit (3,3)-IPUF. The prediction accuracy of the model is around 50% when 200,000 CRPs are used in the training phase (see Table 4).

Unavailability of Derivative Based Machine Learning Attacks on the IPUF: In the analysis of the security of the IPUF against classical ML attacks, we **do not specifically** consider the type of machine learning attack, i.e., black box methods, derivative based white box methods or derivative free white box methods. In Appendix 9.4, we prove that the derivative based white box attacks can at best learn a linear approximated model of the IPUF and therefore reduce to LA-RML or LA-CML.

We already proved that the (x, y)-IPUF with the interposed bit position in the middle is equivalent to a $(y + \frac{x}{2})$-XOR APUF in terms of general security. From Inequality 1, we can say that $(y + \frac{x}{2}) < 10$ to defeat derivative free modeling attacks on a $(y + \frac{x}{2})$-XOR APUF. The number 10 is reported in [TB15], where it is shown that if $(y + \frac{x}{2}) = 10$, then the state-of-the art derivative based machine learning attacks are infeasible on a $(y + \frac{x}{2})$-XOR APUF. This means that IPUFs requires less APUF components than an XOR APUF to be secure. As a result, IPUFs are better in terms of security, reliability and hardware overhead compared to XOR APUFs.

5.3.2 Other (x, y)-IPUF Security Properties

Reliability of the (x, y)-IPUF: We comprehensively study the reliability of (x, y)-IPUF with the results based on the simulation and FPGA implementation IPUF in Appendix 9.7. Over there, we show that the reliability of (x, y)-IPUF is better than that of $(x + y)$-XOR PUF.

Strict Avalanche Property of (x, y)-IPUF and Resistance Against PAC Learning Attacks: The SAC property is an important security feature as discussed in [MKP09, DGSV14, NSCM16]. In Appendix 9.5 we analyze the SAC property of (x, y)-IPUF and then show in Appendix 9.6 that IPUFs are secure against PAC Learning attacks [GTFS16] based on the result of the SAC analysis. We also explain why the PAC learning attacks in [GTS15, GTS16] are not applicable.

6 Simulation Results

We provide simulation results in this section to support the major security and reliability claims made regarding the IPUF.

6.1 IPUF Security

6.1.1 Simulated Machine Learning Attacks On IPUF and XOR APUF

To compare the vulnerabilities of the XOR APUF and various IPUF configurations to machine learning attacks we used the following setup: We simulated a 64-bit 6-XOR APUF, a 64-bit $(1, 1)$-IPUF and a 64-bit $(3, 3)$-IPUF using Matlab. Note that, all the IPUFs have the interposed bit in the middle position.

The APUF components that make up each PUF design use weights that follows a normal distribution with $\mu = 0$ and $\sigma = 0.05$. The noise for each weight follows a normal distribution $\mathcal{N}(0, \sigma^2_{\text{noise}})$. The distribution of each weight is therefore $\mathcal{N}(0, \sigma^2 + \sigma^2_{\text{noise}})$. In our simulations, we used the following relation between σ and σ_{noise} to control the reliability levels: $\sigma_{\text{noise}} = \gamma\sigma$, where $0 \leq \gamma \leq 1$. For $\gamma = 0$, a PUF instance is 100% reliable.

On each respective PUF design we run three different machine learning attacks (two in the case of the XOR APUF). We perform a classical machine learning attack (denoted as

Table 4: Vulnerability of different PUF designs to machine learning attacks. CML=Classical Machine Learning attack, RML=Reliability based Machine Learning attack, LA-RML=Linear Approximation Reliability based Machine Learning attack, LA-CML=Linear Approximation Classical Machine Learning attack.

		PUF Design		
		6-XOR APUF	(1,1)-IPUF	(3,3)-IPUF
Attack	CML	50.2% (✗) [†]	82.4% (✓)[‡]	52.9% (✗)
	RML	84.0% (✓)	N/A(✗)	N/A (✗)
	LA-CML	N/A(✗)	74.0% (✓)	49.0% (✗)
	LA-RML	N/A(✗)	73.0% (✓)	48.0% (✗)

[†] Attack fails
[‡] Attack works

CML in Table 4), the reliability based CMA-ES attack (denoted as RML in Table 4) and the linear approximation to the classical and reliability based machine learning attack (denoted as LA-CML and LA-RML in Table 4).

Each attack in Table 4 is performed using CMA-ES to optimize the mathematical model for 1000 iterations. Each attack uses 200,000 CRPs for training (or 200,000 challenge reliability pairs in the case of the reliability attacks). The accuracy of the attack is computed based on a testing dataset of 2000 CRPs. We compute the accuracies reported in Table 4 by running each attack 10 times and taking the average.

The security of the 6-XOR APUF is shown in Table 4 in the first column. It is clear that an XOR APUF using a large number of APUF components (in this case 6) can mitigate CML attacks, given the amount of training data provided in this setup. However, the 6-XOR APUF is still highly vulnerable to RML attacks. This result is demonstrated in Table 4 as the reliability based CMA-ES attack achieves an average accuracy of 84% on this PUF design. Note that we do not run any attacks on the 6-XOR APUF that use the linear approximation because these types of attacks are specific to the IPUF.

The resilience of the $(1,1)$-IPUF to the CML, LA-CML and LA-RML is shown in column two of Table 4. We note the following: As hypothesized, the $(1,1)$-IPUF is vulnerable to CML due to its low model complexity. However, the linear approximation reliability based CMA-ES attack (LA-RML) works on the $(1,1)$-IPUF which may seem unexpected given our previous claims. Recall that in general the reliability based CMA-ES attack cannot be performed on any IPUF design (hence the X in entry for the RML attack for the $(1,1)$-IPUF). This is because the input to the y-XOR APUF is unknown and therefore Δ cannot be computed. However, in our LA-RML attack on the $(1,1)$-IPUF and $(3,3)$-IPUF we do not use the original formulation of the reliability based CMA-ES attack. To make the attack work on IPUF configurations we assume the interposed bit to be 0. By doing this we can now compute Δ and treat the $(1,1)$-IPUF as a single APUF. In section 5.3.1 we showed that for the $(x,1)$-IPUF using any ML technique with the linear approximation would have an upper bounded model accuracy of 75%. The model accuracy produced by the LA-RML and LA-CML on the $(1,1)$-IPUF in Table 4 closely matches our theoretical upper bound.

The security of the $(3,3)$-IPUF against CML, LA-CML and LA-RML is shown in the third column of Table 4. It can clearly be seen that all attacks fail to produce an accurate model of the $(3,3)$-IPUF. Due to the high model complexity, the $(3,3)$-IPUF is not vulnerable to the CML attack, just like the 6-XOR APUF. Just like for the $(1,1)$-IPUF, the reliability based CMA-ES attack cannot be performed on the $(3,3)$-IPUF. When we run the linear approximation reliability based CMA-ES attack, due to the higher y, the

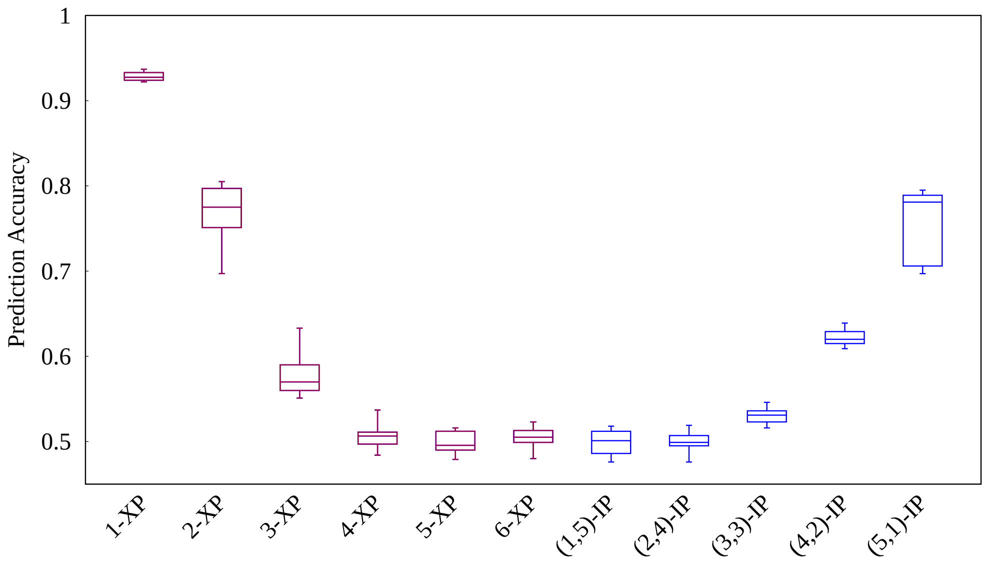

Figure 2: Prediction accuracy of reliability based CMA-ES attack on 64-bit APUF (1-XP), 64-bit 2,3,4,5,6-XOR APUF (y-XP) and (1,5), (2,4), (3,3), (4,2), (5,1)-IPUF ((x,y)-IP).

accuracy of the model generated by any method that uses the linear approximation is theoretically upper bounded at 75% (See Eq. (15)). This coincides with the low accuracy of the model generated by both the linear approximation reliability based CMA-ES attack and the linear approximation CRP based CMA-ES. Overall our experimental results for this section support our claim that the (x, y)-IPUF with proper parameter choices is secure against all current state-of-the-art of machine learning attacks.

6.1.2 (x, y)-IPUF and $(x + y)$-XOR APUF Model Complexity Comparisons

In Section 5.3, we compared the (x, y)-IPUF and the $(x + y)$-XOR APUF. Since we only focus on the design, we consider reliable PUFs to experimentally demonstrate Eq. (20), i.e. If the interposed bit position is in the middle, then the (x, y)-IPUF is equivalent to a $(y + \frac{x}{2})$-XOR APUF (see Appendix 9.3). We run the CMA-ES reliability attack on 64-bit APUF (a.k.a 1-XOR APUF or 1-XP), 64-bit 2,3,4,5,6-XOR APUF (y-XP) and (1,5), (2,4), (3,3), (4,2), (5,1)-IPUF ((x,y)-IP) with 200,000 CRPs for training. In each attack the CMA-ES algorithm is run for 1000 iterations. The results are shown in Fig 2. For each PUF, we attack it 10 times. The prediction accuracy of each attack is computed using 2000 CRPs. Fig 2 shows that the experimental results closely matches the theory presented in Eq. (20).

6.1.3 Requisite APUF components for a secure (x, y)-IPUF

Under state-of-the-art classical ML, the x-XOR APUF must resists both CFW and CDW attacks, the latter requires $x \geq 8$ for 128 bit challenges. Under state-of-the-art classical ML, the IPUF only needs to resist the CFW attack (since known CDW attacks can be prevented) and the equivalence proof shows that this means that $y + x/2$ must be chosen large enough for an $(y + x/2)$-XOR APUF to resist CFW. In this case, see Ineq. (1), $y + x/2$ can be chosen smaller than 10 (because we do not need to resist CDW).

We ran CRP based CMA-ES attacks using CRPs (state-of-the art DW) on different XOR APUF configurations. The attack was repeated 20 times, and each instance of

CMA-ES was run for 2000 iterations. We attacked a 128 bit 4-XOR APUF with 10 million CRPs for training data. We consider using 10 million CRPs which requires 4.5 weeks in our implementation. In 20 attack runs we achieved an average model accuracy of 51.78%. If an adversary wants a high accuracy, then a much larger training set is required taking significantly more time. Essentially this shows a $(1, 4)$-IPUF (5 APUF components) is secure for the 128 bit case.

For 128 bits an XOR APUF requires 8 APUF components, but an IPUF only requires 5. This experiment clearly shows the benefit of the IPUF as it can be secured against CML with fewer APUF components. This results in a smaller hardware footprint and more reliable PUF design.

6.2 IPUF Reliability

Due to the limitation of pages, the study of IPUF reliability based on simulation is provided in Appendix 9.7.

7 IPUF Implementation

In order to validate our IPUF security and reliability claims, we implemented our proposed IPUF designs on an FPGA board. In this section, we describe the FPGA implementation details and related experimental results. We also discuss the limitations of FPGA based APUFs on composite PUF (XOR APUF and IPUF) security.

7.1 IPUF Implementation Details

In our IPUF design we implemented every stage (switch) of each APUF by a Look-Up Table (LUT)[5]. The LUTs are chained together and the final output is collected by a flip-flop serving as an arbiter. The main issue in implementing any IPUF design is to make sure that the response r_{up} of the upper layer XOR APUF is ready when the interposed position of the lower layer XOR APUF is evaluated. To solve this issue, we added one more signal from the upper layer XOR APUF to inform the control circuitry when r_{up} is ready. Once the signal is received the lower layer XOR APUF evaluates its input.

Desirable statistical properties of a PUF FPGA implementation include uniqueness, reliability and uniformity. It has been experimentally verified that uniqueness is a serious issue when implementing FPGA based APUFs [MGS11, HYKS10]. The main reason implementing unique APUFs on FPGAs is problematic [MYIS14, MGS11] is because the designers are not allowed to precisely control the routing between each LUT to maintain the balance of the length of the two competing paths, the delay difference induced by routing is much larger than the delay difference introduced by process variation. Thus, the behavior of one APUF on an FPGA is largely determined by the place and route of the LUTs.

We used two different ways to place the switch chains: (1) Random placement: we randomly select one LUT in each slice and then connect them together. (2) Pattern placement: we place the switches according to a pre-defined pattern. For example, we only use LUT A and LUT B in every slice. Each method has its own strengths and weakness, see Appendices 9.10 and 9.10 for a detailed discussion. Since the design strategy will largely influence the experimental results that we will present later, we will clearly state how the APUFs are generated for each experiment.

[5]In particular on our board, each stage is implemented by a 6-input 2-output LUT, where the two outputs serve as the outputs of upper and lower paths and only three inputs are used as the inputs of upper and lower paths and the challenge bit. We notice that Programmable Delay Line (PDL) is a widely used technique to implement APUFs [MKD10], but we did not choose to use it due to the poor uniqueness of PDL-based APUFs according to a recent study [SCM15].

Table 5: Results of reliability based machine learning attack on XOR APUFs with real measurements from the FPGA.

	#CRPs used in one attack	Overall Noise Rate	Average Prediction Accuracy
2-XOR	50,000	1.44%	98.22%
3-XOR	90,000	2.38%	96.38%
4-XOR	140,000	2.92%	96.15%
5-XOR	200,000	3.80%	96.62%
6-XOR	260,000	4.47%	91.58%*

*Note that, the attack on 6-XOR APUF only recovered 5 out of 6 models.
The attacks on 2,3,4,5 XOR APUFs successfully recovered all the models.

7.2 Experimental Results

Reliability Based Machine Learning Attack on XOR APUFs: First, we repeated the enhanced reliability based CMA-ES attack in Section 9.9 on XOR APUFs to validate the effectiveness of our attack. In this experiment, we selected 6 unique APUFs created by random placement to form a 6-XOR APUF on the FPGA. We then measured 300,000 CRPs with each CRP measurement repeated 11 times to get 300,000 challenge-reliability pairs. The number of challenge-reliability pairs used for one CMA-ES attack and the modeling results after 100 runs of CMA-ES are presented in Table 5.

Reliability Based Machine Learning Attack on IPUFs: To show the modeling resistance of the IPUF to the enhanced reliability based CMA-ES attack, we perform the attack on a (1,1)-IPUF. We do not test this attack on IPUF designs with more APUF components because our security against reliability based machine learning attacks does not depend on the number of APUF components.

We used two APUFs created by pattern placement to form a (1,1)-IPUF with an interposed position exactly in the middle in the lower APUF. We measured 200,000 CRPs with each CRP measurement repeated 11 times to get the challenge-reliability measurements. We then sampled a subset of 90,000 challenge reliability pairs out of the 200,000 challenge-reliability pairs to run the reliability based CMA-ES attack. CMA-ES was not able to converge to the upper APUF after 10 runs. This validated our security claim that IPUF structure can prevent reliability based machine learning attacks. Unfortunately, due to the uniqueness issue of pattern placed APUFs, we were not able to test the security of the (3,3)-IPUF as we did in our experimental simulations. We also observed that if the component APUFs are created by random placement, CMA-ES was able to break it. We give a detailed analysis of this phenomenon in Appendices 9.10 and 9.11. We want to clarify the fact that the reliability based CMA-ES attack can break the IPUF because of the **improper implementation in case of random placement** (see explanation in Appendix 9.11), i.e., **not because of any design flaws of the IPUF**.

Classical Machine Learning Attacks on XOR APUFs and IPUFs: In this subsection we conduct experiments to verify the claim that the model complexity of an (x, y)-IPUF is similar to that of a (y+$\frac{x}{2}$)-XOR APUF. In this experiment we generate component APUFs using the random placement design strategy to construct IPUFs and XOR APUFs.

We measured 200,000 CRPs for each XOR APUF and IPUF. We then used CRP based CMA-ES to optimize each model given the 200,000 CRPs. To further reduce the influence of noisy CRPs in this attack, for each CRP we did a majority voting from 11 repeated measurements. We ran CRP based CMA-ES on this training dataset 10 times to avoid the possible failure introduced by the probabilistic nature of the algorithm. The results

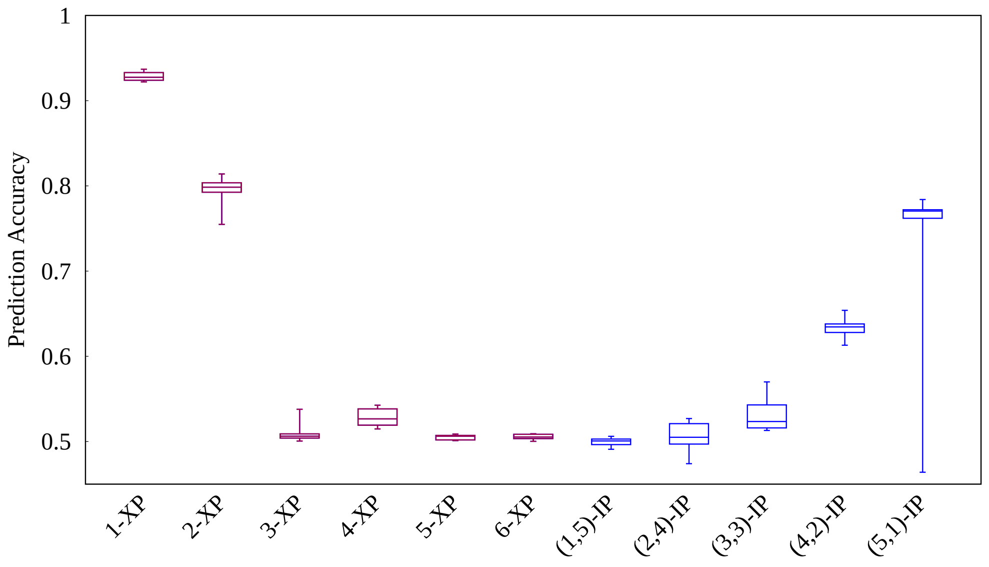

Figure 3: Results of CRP based CMA-ES attacks on APUF (1-XP), x-XOR APUFs (x-XP) and $((x, y))$-IPUFs ((x, y)-IP).

are shown in Fig. 3

Due to the page limit, we provide results on the SAC property results and reliability of the FPGA-implementation of the 64-bit $(3, 3)$-IPUF in Appendices 9.5 and 9.7, respectively.

8 Conclusion

In this paper, we develop three main contributions. First, we comprehensively analyzed reliability based CMA-ES attack to understand how it works and how to enhance it. Second we propose a new PUF design, the (x, y)-IPUF. We prove through theory and experimentation that the IPUF is not vulnerable to the strongest known reliability based machine learning attack (white box derivative free) and the strongest known classical machine learning attack (white box derivative based). Our final contribution is publicly available source code for all our IPUF, XOR APUF and APUF attack simulations written in Matlab and C#. We also provide source code for the FPGA implementation of the XOR APUF and IPUF. Since the IPUF has more advantages in terms of security, reliability and hardware overhead compared to the XOR APUF, **it implies that the IPUF can be considered a standard design or primitive replacement for the XOR APUF**. As a next step, we propose to implement the IPUF in ASIC in order to overcome the uniqueness problem encountered in FPGA implementations.

Acknowledgment

This project was supported in part by the AFOSR MURI under award number FA9550-14-1-0351. Ulrich Rührmair gratefully acknowledges funding by the PI-COLA project of the German Bundesministerium für Bildung und Forschung (BMBF).

References

[Bec14] Georg T. Becker. On the Pitfalls of using Arbiter-PUFs as Building Blocks. *IACR Cryptology ePrint Archive*, 2014:532, 2014.

[Bec15] Georg T. Becker. The Gap Between Promise and Reality: On the Insecurity of XOR Arbiter PUFs. In *Proc. of 17th International Workshop on Cryptographic Hardware and Embedded Systems (CHES)*, 2015.

[BFSK11] Christina Brzuska, Marc Fischlin, Heike Schrauder, and Stefan Katzenbeisser. Physically Uncloneable Functions in the Universal Composition Framework. In Phillip Rogaway, editor, *CRYPTO*, pages 51–70. 2011.

[CCL$^+$11] Qingqing Chen, G. Csaba, P. Lugli, U. Schlichtmann, and U. R ührmair. The Bistable Ring PUF: A new architecture for strong Physical Unclonable Functions. In *Proc. of IEEE International Symposium on Hardware-Oriented Security and Trust (HOST)*, pages 134 –141, june 2011.

[DGSV14] Jeroen Delvaux, Dawu Gu, Dries Schellekens, and Ingrid Verbauwhede. Secure Lightweight Entity Authentication with Strong PUFs: Mission Impossible? In *Proc. of 16th International Workshop on Cryptographic Hardware and Embedded Systems (CHES)*, pages 451–475, 2014.

[Dig16] Digilent. Nexys 4 DDR Reference Manual, Apr. 2016. [Accessed Feb., 2018].

[DRS04] Yevgeniy Dodis, Leonid Reyzin, and Adam Smith. Fuzzy Extractors: How to Generate Strong Keys from Biometrics and Other Noisy Data. In Christian Cachin and Jan L. Camenisch, editor, *EUROCRYPT*, pages 523–540. 2004.

[DV13] J. Delvaux and I. Verbauwhede. Side Channel Modeling Attacks on 65nm Arbiter PUFs Exploiting CMOS Device Noise. In *IEEE 6th Int. Symposium on Hardware-Oriented Security and Trust* , 2013.

[GCvDD02] Blaise Gassend, Dwaine Clarke, Marten van Dijk, and Srinivas Devadas. Silicon physical random functions. In *ACM CCS*, 2002.

[GTFS16] Fatemeh Ganji, Shahin Tajik, Fabian Fäßler, and Jean-Pierre Seifert. Strong Machine Learning Attack against PUFs with No Mathematical Model. In *CHES*, pages 391–411. Springer Berlin Heidelberg, 2016.

[GTS15] Fatemeh Ganji, Shahin Tajik, and Jean-Pierre Seifert. Why attackers win: on the learnability of XOR arbiter PUFs. In *International Conference on Trust and Trustworthy Computing*, pages 22–39. Springer International Publishing, 2015.

[GTS16] Fatemeh Ganji, Shahin Tajik, and Jean-Pierre Seifert. PAC learning of arbiter PUFs. *Journal of Cryptographic Engineering*, 6(3):249–258, 2016.

[HAP09] Ryan Helinski, Dhruva Acharyya, and Jim Plusquellic. A physical unclonable function defined using power distribution system equivalent resistance variations. In *Proc. of 46th Annual Design Automation Conference(DAC)*, pages 676–681, New York, NY, USA, 2009. ACM.

[HYKS10] Y. Hori, T. Yoshida, T. Katashita, and A. Satoh. Quantitative and Statistical Performance Evaluation of Arbiter Physical Unclonable Functions on FPGAs. In *Proceedings of International Conference on Reconfigurable Computing and FPGAs (ReConFig)*, pages 298 –303, dec. 2010.

[JHR+17] Chenglu Jin, Charles Herder, Ling Ren, Phuong Ha Nguyen, Benjamin Fuller, Srinivas Devadas, and Marten van Dijk. FPGA Implementation of a Cryptographically-Secure PUF Based on Learning Parity with Noise. *Cryptography*, 1(3):23, 2017.

[KGM+08] S.S. Kumar, J. Guajardo, R. Maes, G.-J. Schrijen, and P. Tuyls. Extended abstract: The butterfly PUF protecting IP on every FPGA. In *HOST*, pages 67–70, June 2008.

[Lim04] Daihyun Lim. Extracting Secret Keys from Integrated Circuits. Master's thesis, MIT, USA, 2004.

[LLG+05] Daihyun Lim, Jae W. Lee, Blaise Gassend, G. Edward Suh, Marten van Dijk, and Srini Devadas. Extracting secret keys from integrated circuits. *IEEE Transactions on Very Large Scale Integration (VLSI) Systems*, 13(10):1200–1205, October 2005.

[LP14] Yingjie Lao and Keshab K. Parhi. Statistical Analysis of MUX-Based Physical Unclonable Functions. *IEEE Trans. on CAD of Integrated Circuits and Systems*, 33(5):649–662, 2014.

[MGS11] Abhranil Maiti, Vikash Gunreddy, and Patrick Schaumont. A Systematic Method to Evaluate and Compare the Performance of Physical Unclonable Functions. *IACR Cryptology ePrint Archive*, 2011:657, 2011.

[MKD10] Mehrdad Majzoobi, Farinaz Koushanfar, and Srinivas Devadas. Fpga puf using programmable delay lines. In *Information Forensics and Security (WIFS), 2010 IEEE International Workshop on*, pages 1–6. IEEE, 2010.

[MKP08] M. Majzoobi, F. Koushanfar, and M. Potkonjak. Testing Techniques for Hardware Security. In *Proc. of IEEE International Test Conference(ITC)*, pages 1–10, Oct. 2008.

[MKP09] Mehrdad Majzoobi, Farinaz Koushanfar, and Miodrag Potkonjak. Techniques for Design and Implementation of Secure Reconfigurable PUFs. *ACM Trans. Reconfigurable Technol. Syst.*, 2(1):1–33, 2009.

[MV10] Roel Maes and Ingrid Verbauwhede. Physically Unclonable Functions: A Study on the State of the Art and Future Research Directions. In Ahmad-Reza Sadeghi and David Naccache, editors, *Towards Hardware-Intrinsic Security*, Information Security and Cryptography, pages 3–37. Springer, Berlin Heidelberg, 2010.

[MYIS14] Takanori Machida, Dai Yamamoto, Mitsugu Iwamoto, and Kazuo Sakiyama. A New Mode of Operation for Arbiter PUF to Improve Uniqueness on FPGA. In *Proc. of Federated Conference on Computer Science and Information Systems (FedCSIS)*, pages 871–878, 2014.

[NSCM16] Phuong Ha Nguyen, Durga Prasad Sahoo, Rajat Subhra Chakraborty, and Debdeep Mukhopadhyay. Security Analysis of Arbiter PUF and Its Lightweight Compositions Under Predictability Test. *ACM TODAES*, 22(2):20, 2016.

[RJB+11] U. Rührmair, C. Jaeger, M. Bator, M. Stutzmann, P. Lugli, and G. Csaba. Applications of High-Capacity Crossbar Memories in Cryptography. *IEEE Transactions on Nanotechnology*, 10(3):489 –498, may 2011.

[RSS+10] Ulrich Rührmair, Frank Sehnke, Jan Sölter, Gideon Dror, Srinivas Devadas, and Jürgen Schmidhuber. Modeling attacks on physical unclonable functions. In *Proc. of 17th ACM conference on Computer and communications security(CCS)*, pages 237–249, New York, NY, USA, 2010. ACM.

[RXS+14] Ulrich Rührmair, Xiaolin Xu, Jan Sölter, Ahmed Mahmoud, Mehrdad Majzoobi, Farinaz Koushanfar, and Wayne P. Burleson. Efficient Power and Timing Side Channels for Physical Unclonable Functions. In *Proc. of 16th International Workshop on Cryptographic Hardware and Embedded Systems (CHES)*, pages 476–492, 2014.

[SCM15] Durga Prasad Sahoo, Rajat Subhra Chakraborty, and Debdeep Mukhopadhyay. Towards ideal arbiter puf design on xilinx fpga: A practitioner's perspective. In *Digital System Design (DSD), 2015 Euromicro Conference on*, pages 559–562. IEEE, 2015.

[SD07] G. Edward Suh and Srinivas Devadas. Physical unclonable functions for device authentication and secret key generation. In *DAC*, pages 9–14, 2007.

[SH14] Dieter Schuster and Robert Hesselbarth. Evaluation of Bistable Ring PUFs Using Single Layer Neural Networks. In *Trust and Trustworthy Computing - 7th International Conference, TRUST 2014, Heraklion, Crete, Greece, June 30 - July 2, 2014. Proceedings*, pages 101–109, 2014.

[SNMC15] Durga Prasad Sahoo, Phuong Ha Nguyen, Debdeep Mukhopadhyay, and Rajat Subhra Chakraborty. A Case of Lightweight PUF Constructions: Cryptanalysis and Machine Learning Attacks. *IEEE TCAD*, 2015.

[Söl09] Jan Sölter. Cryptanalysis of Electrical PUFs via Machine Learning Algorithms. Master's thesis, Technische Universität München, 2009.

[TB15] Johannes Tobisch and Georg T. Becker. On the Scaling of Machine Learning Attacks on PUFs with Application to Noise Bifurcation. In *Proc. of 11th International Workshop on Radio Frequency Identification: Security and Privacy Issues (RFIDsec)*, pages 17–31, 2015.

[TDF+14] Shahin Tajik, Enrico Dietz, Sven Frohmann, Jean-Pierre Seifert, Dmitry Nedospasov, Clemens Helfmeier, Christian Boit, and Helmar Dittrich. Physical Characterization of Arbiter PUFs. In *Cryptographic Hardware and Embedded Systems - CHES 2014 - 16th International Workshop, Busan, South Korea, September 23-26, 2014. Proceedings*, pages 493–509, 2014.

[TLG+15] S. Tajik, H. Lohrke, F. Ganji, J. P. Seifert, and C. Boit. Laser Fault Attack on Physically Unclonable Functions. In *12th Workshop on Fault Diagnosis and Tolerance in Cryptography (FTDC)*, 2015.

[WGM+17] Nils Wisiol, Christoph Graebnitz, Marian Margraf, Manuel Oswald, Tudor Soroceanu, and Benjamin Zengin. Why Attackers Lose: Design and Security Analysis of Arbitrarily Large XOR Arbiter PUFs. 2017.

[XRHB15] Xiaolin Xu, Ulrich Rührmair, Daniel E. Holcomb, and Wayne P. Burleson. Security Evaluation and Enhancement of Bistable Ring PUFs. In *Proc. of 11th International Workshop on Radio Frequency Identification: Security and Privacy Issues (RFIDsec)*, pages 3–16, 2015.

[YKL+13] Yida Yao, Myung-Bo Kim, Jianmin Li, Igor L. Markov, and Farinaz Koushanfar. ClockPUF: Physical Unclonable Functions based on Clock Networks. In *Design, Automation & Test in Europe (DATE)*, Grenoble, France, 2013.

[YMSD11] Meng-Day (Mandel) Yu, David M'Raïhi, Richard Sowell, and Srinivas Devadas. Lightweight and Secure PUF Key Storage Using Limits of Machine Learning. In *CHES*, pages 358–373, 2011.

9 appendix

9.1 Description of APUFs and XOR APUFs

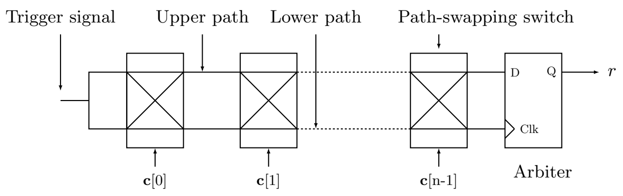

Figure 4: Arbiter PUF.

We briefly introduce the design of Arbiter PUFs (APUFs) and the reader is referred to [GCvDD02] for further details. The design of an APUF is depicted in Fig. 4. It is a delay-based silicon PUF with n-bit challenge $\mathbf{c} = (\mathbf{c}[0], \mathbf{c}[1], \ldots, \mathbf{c}[n-1])$ that extracts random variation in silicon in terms of the delay difference of two symmetrically laid out parallel delay lines. Ideally, the nominal delay difference between these path pairs should be 0, but this does not happen due to uncontrollable random variation in the manufacturing process that introduces random offset between the two path delays. In general, an n-bit APUF comprises of n switches connected serially to build two distinct, but symmetrical paths. The arbiter which is located at the end of the two paths is used to decide which path is faster. The challenge bits $\mathbf{c}[0], \mathbf{c}[1], \ldots, \mathbf{c}[n-1]$ are used as the control input of path-swapping switches that eventually results in two paths and input stimulus runs through these two paths. The arbiter declares which path wins the race in the form of a 0 or 1 response. Typically, the response of an APUF is defined by

$$r = \begin{cases} 1, & \text{if the signal at the upper path runs faster} \\ 0, & \text{otherwise.} \end{cases}$$

The most important feature of this design is its small hardware overhead, i.e. the hardware overhead of an n-bit APUF is linearly proportional to the number of challenge bits n.

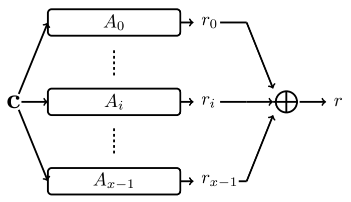

Figure 5: x-XOR APUF.

Due to the existence of a linear addative delay model of the APUF, see Eq(2), a modeling attack is applicable [LLG$^+$05, RSS$^+$10]. In [SD07], the authors proposed the design of an x-XOR APUF which enjoys better modeling resistance. Figure 5 describes the design of an x-XOR APUF.

9.2 Proof of Influence of Challenge Bit $\mathrm{c}[j]$ on the Response r in the APUF

In this section, we prove

$$\Pr_{\mathbf{c}}(r_{\mathbf{c}[j]=0} = r_{\mathbf{c}[j]=1}) \approx \frac{(n-j)}{n}, j = 0, \ldots, n-1.$$

Let us examine under which conditions $r_{\mathbf{c}[j]=0}$ will equal $r_{\mathbf{c}[j]=1}$. Assume for a specific challenge $\mathbf{c}$ we fix all bits (except for $\mathbf{c}[j]$) and the output r is 0 regardless of the value of $\mathbf{c}[j]$. This means $\Delta_{\mathbf{c}[j]=0} = \Delta_{Flipping} + \Delta_{Non-Flipping} > 0$ when $\mathbf{c}[j] = 0$ and $\Delta_{\mathbf{c}[j]=1} = -\Delta_{Flipping} + \Delta_{Non-Flipping} > 0$ when $\mathbf{c}[j] = 1$. From this example, it is easy to derive that if and only if $r_{\mathbf{c}[j]=0} = r_{\mathbf{c}[j]=1}$, then $|\Delta_{Flipping}| \leq |\Delta_{Non-Flipping}|$ so that:

$$\Pr_{\mathbf{c}}(r_{\mathbf{c}[j]=0} = r_{\mathbf{c}[j]=1}) = \Pr(|\Delta_{Flipping}| \leq |\Delta_{Non-Flipping}|). \tag{16}$$

We follow existing PUF literature [Lim04, LP14] and assume that when generating an instance of an APUF all $\mathbf{w}_i$ are sampled from the same normal distribution $\mathcal{N}(0, \sigma^2)$ and hence, $\Delta_{Flipping} \sim \mathcal{N}(0, (j+1) \times \sigma^2)$ and $\Delta_{Non-Flipping} \sim \mathcal{N}(0, (n-j) \times \sigma^2)$. Thus $\Pr_{\mathbf{c}}(r_{\mathbf{c}[j]=0} = r_{\mathbf{c}[j]=1})$ is equal to:

$$\begin{aligned} &= \Pr(|\Delta_{Flipping}| \leq |\Delta_{Non-Flipping}|) \qquad (17) \\ &= 4 \times \int_0^{\infty} \phi_{0,(n-j)\sigma^2}(u)\Phi_{0,(j+1)\sigma^2}(-u)du, \end{aligned}$$

where $\phi_{\mu,\sigma^2}(\cdot)$ and Φ_{μ,σ^2} are the probability distribution function and cumulative distribution function of a normal distribution $\mathcal{N}(\mu, \sigma^2)$, respectively. Experimentally it has been shown [MKP09, DGSV14, NSCM16] that Eq. (17) can be approximated as:

$$\Pr_{\mathbf{c}}(r_{\mathbf{c}[j]=0} = r_{\mathbf{c}[j]=1}) \approx \frac{(n-j)}{n}, j = 0, \ldots, n-1.$$

9.3 The Relationship between (x, y)-IPUF and $(x + y)$-XOR APUF

We prove that if the interposed bit position is i, then the (x, y)-IPUF is equivalent to the $(y + p_r x)$-XOR APUF where

$$p_r = \frac{1-(1-2p)^y}{2} \qquad \text{and} \qquad p = \frac{i}{n}.$$

For a fixed challenge we study the contribution of each APUF component of an x-XOR APUF to the output of the XOR APUF. Here we define **contributes** in the following manner. If we flip the output of APUF A_i (while the rest of the APUF outputs are held constant) and this causes the final response of the PUF r to flip, then we say that A_i **contributes** to the output for a challenge $\mathbf{c}$. In an x-XOR APUF it can clearly be seen that each of the x APUFs contribute to the output. This is because in an XOR gate flipping any one of the inputs always causes the output to flip. We know the more APUFs that contribute to the output, the harder the XOR APUF design is to attack with classical machine learning.

Now we will analyze the (x, y)-IPUF to see how many APUFs contribute to the output (essentially how difficult it is to attack with classical machine learning). We denote r_y^0 as the output of the IPUF when $r_x = 0$ with $\mathbf{c}_y = (\mathbf{c}[0], \ldots, \mathbf{c}[i], r_x = 0, \mathbf{c}[i+1], \ldots, \mathbf{c}[n-1])$ and r_y^1 as the output of the IPUF when $r_x = 1$ with $\mathbf{c}_y = (\mathbf{c}[0], \ldots, \mathbf{c}[i], r_x = 1, \mathbf{c}[i+1], \ldots, \mathbf{c}[n-1])$. Based on our definition of contribution above, if $r_y^0 = r_y^1$ it means that the x-XOR APUF output r_x does not contribute to the final output r_y of the IPUF. In this case only y APUFs contribute to the output of the IPUF.

Note we can also write $r_y^0 = r_y^1$ as $r_y^1 \oplus r_y^0 = 0$. Alternatively if $r_y^1 \oplus r_y^0 = 1$ then the output of (x, y)-IPUF depends on the output r_x of x-XOR PUF, as well as the output r_y of the y-XOR PUF. This implies that there are $(x + y)$ APUFs which contribute to the final output r_y for a given challenge. Therefore, the challenge-response space of an (x, y)-IPUF can be partitioned into two groups. The first group represents challenge-response pairs where the response only depends on the y APUFs of the y-XOR PUF. The second group of challenge-response pairs has responses which depend on both the x-XOR APUF and the y-XOR APUF (the response depends on a total of $(x + y)$ APUFs). Now we calculate the expected number of challenge-response pairs in each group. First, we will compute the probability the challenge-response pair is in the second group:

$$p_r = \Pr_{\mathbf{c}}(r_y^0 \neq r_y^1) = \Pr_{\mathbf{c}}(r_y^0 \oplus r_y^1 = 1) \tag{18}$$

Let $r_{low,0}, r_{low,1}, \ldots, r_{low,y-1}$ be the outputs of the y APUFs in the lower layer y-XOR PUF when r_x is 0. We will assume ideal classical machine learning conditions where no measurement noise is present. Because there is no measurement noise Section 5.1 is applicable: For a given challenge $\mathbf{c}$, $r_{low,i}$ depends on the upper layer output r_x (in that output $r_{low,i}$ would flip if r_x would be substituted by 1) with probability $p = (i+1)/(n+1) \approx i/n$ if the feedback position of r_x is i. For a given challenge $\mathbf{c}$, p_r is the probability that the response of (x, y)-IPUF is equal to $r = 1 \oplus r_{low,0} \oplus \ldots \oplus r_{low,y-1}$ if r_x would be substituted by 1. Then p_r depends on i:

$$p_r = \sum_{k=1, k \text{ odd}}^{y} \binom{y}{k} p^k (1-p)^{y-k} = \frac{1 - (1-2p)^y}{2}. \tag{19}$$

Thus, a fraction $1 - p_r$ of challenge-response pairs is in the first group and a fraction p_r of challenge-response pairs is in the second group. For a given (x, y)-IPUF with parameter i, the *expected* number of APUFs contributing to the response of a given challenge is

$$\begin{aligned} &= (1 - p_r)y + p_r(x + y) \\ &= y + p_r x \end{aligned} \tag{20}$$

9.4 Proof of Unavailability of Derivative Based ML Attacks on the IPUF

As discussed in Section 1, the white-box machine learning techniques can be partitioned into two different categories: *derivative based modeling attacks* and *derivative free modeling attacks*. Basically, the former works more efficiently than the latter one when the searching space is large. For example, in [TB15], using Logistic Regression we can successfully model 4-XOR APUF with 15,000 CRPs only while using CMA-ES we cannot have a good model for 4-XOR APUF with 200,000 CRPs (see Figure 2). Hence, it is important to know if there exists any possible derivative based modeling attacks (CDW) on the IPUF or not. We show that the answer to this question is **NO** by analyzing Logistic Regression (LR), i.e., the state-of-the-art CDW.

In the upper x-XOR APUF of the IPUF, since there are x n-bit APUF instances, we denote $\mathbf{w}^x = (\mathbf{w}_1^x, \ldots, \mathbf{w}_x^x)$ as the model of the x-XOR APUF. Futher we denote $\mathbf{w}_i^x = (\mathbf{w}_i^x[0], \ldots, \mathbf{w}_i^x[n])$ as the $(n+1)$ dimensional vectors and the models of the APUFs in the x-XOR APUF, $i = 1, \ldots, x$. Similarly, $\mathbf{w}^y = (\mathbf{w}_1^y, \ldots, \mathbf{w}_y^y)$ is the model of the y-XOR APUF of the IPUF and $\mathbf{w}_i^y$ are $(n+2)$ dimensional vectors and the models of APUFs in the y-XOR APUF. In order to enable derivative based ML attacks, we follow the approach proposed in [RSS+10, Söl09] (this is the Logistic Regression ML attack on an x-XOR APUF), i.e. we approximate the discrete output r_x and r_y by a continuous function sigmoid $\sigma(\cdot)$ where $\sigma(x) = \frac{1}{1+\exp(-x)}$. More precisely, we define the following functions (here $\mathbf{\Phi}(\mathbf{c}, \hat{r}_x)$ denotes $\mathbf{\Phi}(.)$ applied to challenge $\mathbf{c}$ interposed with $\hat{r}_x$):

$$\begin{aligned}
\Delta_x &= g_x(\mathbf{w}^x, \mathbf{c}) = \prod_{i=1}^{x} \langle \mathbf{w}_i^x, \mathbf{\Phi}(\mathbf{c}) \rangle, \\
r_x &= \delta(\Delta_x) = \delta(g_x(\mathbf{w}^x, \mathbf{c})), \\
\hat{r}_x &= \delta(\Delta_x) + e(\Delta_x) = \delta(g_x(\mathbf{w}^x, \mathbf{c})) + e(g_x(\mathbf{w}^x, \mathbf{c})), \\
\Delta_y &= g_y(\mathbf{w}^y, \mathbf{c}, \hat{r}_x) = \prod_{i=1}^{y} \langle \mathbf{w}_i^y, \mathbf{\Phi}(\mathbf{c}, \hat{r}_x) \rangle, \\
\hat{r}_y &= \sigma(\Delta_y) = \sigma(g_y(\mathbf{w}^x, \mathbf{c}, \hat{r}_y)),
\end{aligned}$$

where $\delta(x)$ is the step function, i.e., $\delta(x) = 0$ if $x > 0$, and $\delta(x) = 0$ otherwise, and e is a certain error function chosen by adversary. The function δ has derivative of 0 everywhere except $x = 0$ (where the derivative is ∞) and $e(x)$ has derivative everywhere. Since in practice Δ_x is never exactly equal to 0, we may assume that the derivative of δ in Δ_x is always equal to 0.

In order to find the optimal solution of $\mathbf{w} = (\mathbf{w}^x, \mathbf{w}^y)$ (i.e. the model for the (x, y)-IPUF) from a randomly generated model $\mathbf{w}$, we define the following function as described in [RSS+10, Söl09]:

$$l = -\frac{1}{N} \sum_{(\mathbf{c}_i, r_i), i=1,\ldots,N} \ln(\sigma(\Delta_y)^{r_i}(1 - \sigma(\Delta_y))^{1-r_i})$$

where $\{(\mathbf{c}_1, r_1), \ldots, (\mathbf{c}_N, r_N)\}$ are the challenge-response pairs of the IPUF in the training set. After that, we need to compute the gradient of l in order to find the optimal solution, i.e., we need to compute

$$\begin{aligned}
\nabla l =& (\frac{\partial l}{\partial \mathbf{w}_1^x[0]}, \ldots, \frac{\partial l}{\partial \mathbf{w}_1^x[n]}, \ldots, \frac{\partial l}{\partial \mathbf{w}_x^x[0]}, \ldots, \frac{\partial l}{\partial \mathbf{w}_x^x[n]}, \\
& \frac{\partial l}{\partial \mathbf{w}_1^y[0]}, \ldots, \frac{\partial l}{\partial \mathbf{w}_1^y[n]}, \ldots, \frac{\partial l}{\partial \mathbf{w}_y^y[0]}, \ldots, \frac{\partial l}{\partial \mathbf{w}_y^y[n]})
\end{aligned}$$

After that we will update $\mathbf{w} = \mathbf{w} - \eta \nabla l$ where η is the learning stepsize. By updating like this many times, we hope that the algorithm will converge to an optimal solution $\mathbf{w}^*$. Now, we focus on the calculation $\frac{\partial l}{\partial \mathbf{w}_i^x[j]}$ which is equal to:

$$\begin{aligned}
&= \partial(-\frac{1}{N} \sum_{(\mathbf{c}_i, r_i), i=1,\ldots,N} \ln(\sigma(\Delta_y)^{r_i}(1 - \sigma(\Delta_y))^{1-r_i}))/\partial \mathbf{w}_i^x[j] \\
&= -\frac{1}{N} \sum_{(\mathbf{c}_i, r_i), i=1,\ldots,N} [r_i(1 - \sigma(\Delta_y)) - (1 - r_i)\sigma(\Delta_y)] \frac{\partial \Delta_y}{\partial \mathbf{w}_i^x[j]}
\end{aligned}$$

We have

$$\begin{aligned}
\frac{\partial \Delta_y}{\partial \mathbf{w}_i^x[j]} = \frac{\partial g_y}{\partial \mathbf{w}_i^x[j]} &= \frac{\partial g_y}{\partial[\delta(\Delta_x) + e(\Delta_x)]} \frac{\partial[\delta(\Delta_x) + e(\Delta_x)]}{\partial \mathbf{w}_i^x[j]} \\
&= \frac{\partial g_y}{\partial[\delta(\Delta_x) + e(\Delta_x)]} \frac{\partial e(\Delta_x)}{\partial \Delta_x} \frac{\partial \Delta_x}{\partial \mathbf{w}_i^x[j]}
\end{aligned}$$

(since $\delta'(\Delta_x) = 0$ as explained above).

But if we consider using the linear approximation with this attack where we fix $\hat{r}_x = 0 + e(\Delta_x)$, then we also have the same result, i.e.,

$$\frac{\partial \Delta_y}{\partial \mathbf{w}_i^x[j]} = \frac{\partial g_y}{\partial[\delta(\Delta_x) + e(\Delta_x)]} \frac{\partial e(\Delta_x)}{\partial \Delta_x} \frac{\partial \Delta_x}{\partial \mathbf{w}_i^x[j]},$$

since Δ_x is exactly equal to 0 with probability 0 and outside $\Delta_x = 0$, $\delta(\Delta_x)$ has derivative 0.

This fact implies that we cannot distinguish the partial derivative of the IPUF from that of the linear approximated model of the IPUF. From this analysis, we conclude that derivative based ML attacks are equivalent to derivative based ML attacks that use the linear approximation. Due to this fact, the IPUF can mitigate derivative based ML attacks just like it can mitigate attacks that use the linear approximation by choosing $y \geq 2$ (as explained in Section 5.3).

9.5 Strict Avalanche Property of (x, y)-IPUF

The SAC property is an important security feature as discussed in [MKP09, DGSV14, NSCM16]. Here we analyze the SAC property of the (x, y)-IPUF. Assume that the output r_x of the x-XOR APUF is interposed at position j in the challenge to the y-XOR APUF, $j = 0, 1, \ldots, n$. We would like to compute the probability that flipping a bit in the input results in the flipping of the output bit of the (x, y)-IPUF. This analysis for the (x, y)-IPUF is similar to the analysis we did for the APUF in Section 5.1:

$$p_i = \Pr_{\mathbf{c}}(r_{c[i]=0} \neq r_{c[i]=1}), i = 0, 1, \ldots, n-1 \tag{21}$$

where $r_{c[i]=0}$ and $r_{c[i]=1}$ are the output of (x, y)-IPUF when bit $\mathbf{c}[i] = 0$ and $\mathbf{c}[i] = 1$, respectively. To compute p_i, we consider the following two cases:

Case I. $\mathbf{c}[i]$ flips, r_x does not flip, r flips. In this case, we flip challenge bit $\mathbf{c}[i]$ but the output r_x of x-XOR APUF does not flip and the (x, y)-IPUF's output r flips (i.e., $r_{c[i]=0} \neq r_{c[i]=1}$). From the analysis in Section 5.1, we know that if the challenge bit $\mathbf{c}[i]$ flips, then the output of an APUF in an x-XOR APUF will flip with expected probability $p = \frac{i}{n}$ and thus, the output of x-XOR APUF will flip with an expected probability $p_x = \frac{1-(1-2p)^x}{2}$. In other words, r_x will not flip with a probability $\bar{p}_x = 1 - p_x = \frac{1+(1-2p)^x}{2}$. When r_x is not flipped due to $\mathbf{c}[i]$ flipping, the output of an APUF in the y-XOR APUF will be flipped by flipping $\mathbf{c}[i]$ with a probability $p' = \frac{i}{n+1}$. Thus the probability that r_x does not flip (and r flips) when flipping $\mathbf{c}[i]$ is equal to:

$$p_I = \frac{1 + (1-2p)^x}{2} \cdot \frac{1 - (1-2p')^y}{2}.$$

Case II. $\mathbf{c}[i]$ flips, r_x flips and r flips. If r_x flips because $\mathbf{c}[i]$ flips, then there are two flipping challenge bits at position i and j in the input challenge to the y-XOR APUF. In this case, the output of an APUF in the y-XOR APUF will be flipped with a probability $p'' = \frac{|i-j|}{n+1}$. The computation for p'' is beyond the scope of this paper but a detailed derivation of it can be found in [NSCM16]. Thus the output r will flip with a probability

$$p_{II} = \frac{1 - (1-2p)^x}{2} \cdot \frac{1 - (1-2p'')^y}{2}$$

Therefore, we have

$$\begin{aligned} p_i =& p_I + p_{II} \\ =& \frac{1 + (1-2p)^x}{2} \cdot \frac{1 - (1-2p')^y}{2} \\ &+ \frac{1 - (1-2p)^x}{2} \cdot \frac{1 - (1-2p'')^y}{2} \\ =& \frac{1 + (1-2\frac{i}{n})^x}{2} \cdot \frac{1 - (1-2\frac{i}{n+1})^y}{2} \\ &+ \frac{1 - (1-2\frac{i}{n})^x}{2} \cdot \frac{1 - (1-2\frac{|i-j|}{n})^y}{2} \end{aligned} \tag{22}$$

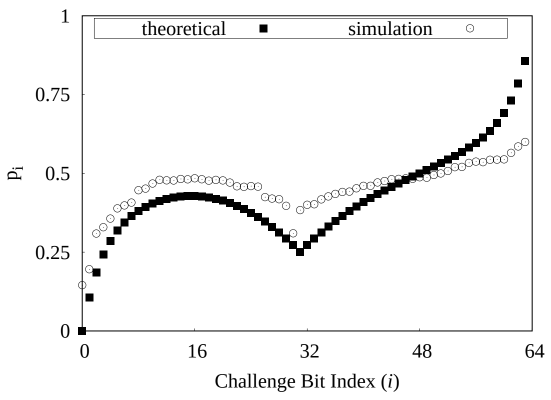

Figure 6: SAC property of 64-bit (3,3)-IPUF with real and simulation data.

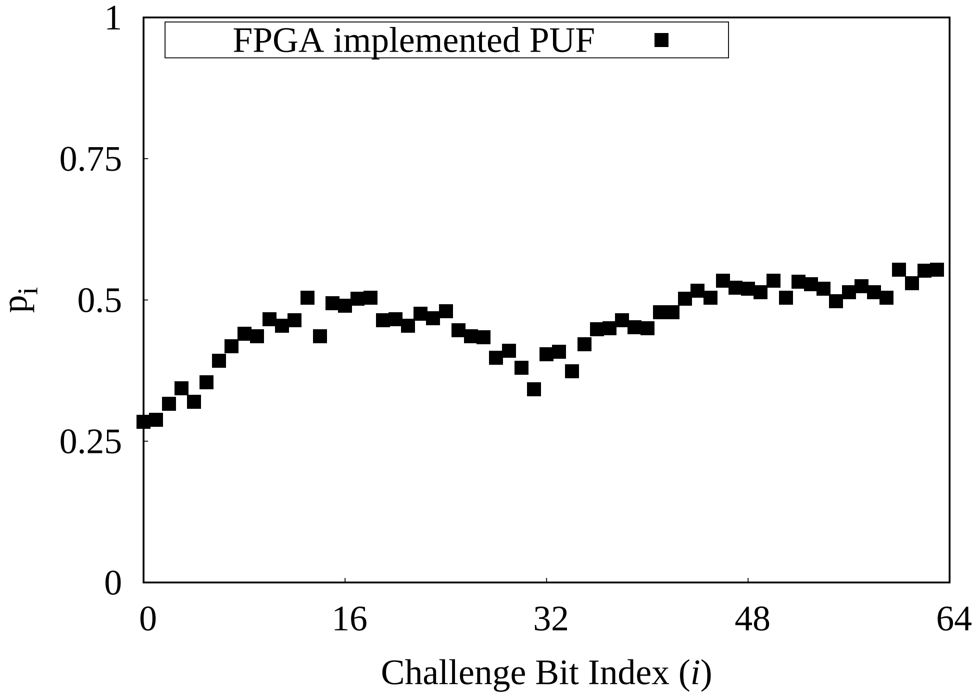

Figure 7: SAC property of 64-bit (3,3)-IPUF with real data.

We experimentally verify our calculations for the SAC property of the $(3,3)$-IPUF and the result is described in Fig 6. The simulation of the SAC property is computed by using 20,000 pairs of CRP for computing each p_i.

We also tested SAC property of an implemented (3,3)-IPUF, where each component APUF is generated by random placement (see Section 7.1). The shape is shown in Figure 7, which is similar to Figure 6.

9.6 PAC Learning Resistance of IPUF

In [GTS15, GTS16, GTFS16], the authors proposed a novel modeling attack based on the PAC learning problem. PAC learning attacks can be divided into two categories: black box attack [GTFS16] and derivative based white box attacks [GTS15, GTS16].

The attack described in [GTFS16] does not work for the IPUF because of the following reason. As described in [GTFS16], assume that if the PUF has k number of *influential bits* (see [GTFS16] for the detailed definition), then this PUF can be ϵ-approximated by another Boolean function h depending on only a constant number of Boolean variables K, where

$$K = e^{\frac{k}{\epsilon}\times(2+\sqrt{\frac{2\epsilon\log_2(4k/\epsilon)}{k}})} > e^{\frac{2k}{\epsilon}}.$$

As shown in [GTFS16], for a n-bit (x, y)-IPUF with interposed position j, k can be computed as follows:

$$k = \sum_{i=0, i\neq j}^{n} p_i \overset{Eq.(22)}{=} \sum_{i=0, i\neq j}^{n} \{ \frac{1 + (1 - 2\frac{i}{n})^x}{2} \frac{1 - (1 - 2\frac{i}{n+1})^y}{2} + \frac{1 - (1 - 2\frac{i}{n})^x}{2} \frac{1 - (1 - 2\frac{|i-j|}{n})^y}{2} \}.$$

For 64-bit $(3, 3)$-IPUF with interpose position $j = 31$, $k = 25.2$. Hence, even if we consider a very weak approximated function h with $\epsilon = 0.5$, then $K = e^{25.2\times2/0.5} > e^{100} > 2^{100}$. It implies that it is impossible to launch the attack proposed in [GTFS16] on a 64-bit IPUF.

The attacks in [GTS15, GTS16] do not apply to IPUF because of the following two reasons.

First reason. The attacks in [GTS15, GTS16] use the perceptron algorithm to learn the model $\mathbf{w}$ of the APUF and XOR APUF. For a given CRP, the weight vector $\mathbf{w}$ will be updated based on the error between the given response and predicted response (see the description of the perceptron algorithm in [GTS15]). The calculated error can be considered as the *gradient* and based on the computed gradient, the weight vector $\mathbf{w}$ is updated. In Appendix 9.4, we already prove that the derivative based white box attacks are not applicable to IPUF. This implies that the attacks in [GTS15, GTS16] do not work for the IPUF when x and y are properly chosen.

Second reason. As pointed out in [GTS15, GTS16], the number of CRPs needed in this type of attack is very sensitive to the length n of a challenge and x, the number of APUFs in the x-XOR APUF. For $x \geq 5$ and $n \geq 64$, the exponential dependency on x and n makes it infeasible to apply this attack to the n-bit x-XOR APUF. As shown in Appendix 9.3, the (x, y)-IPUF is equivalent to the $(y + x/2)$-XOR APUF under classical ML. Therefore, the attacks in [GTS15, GTS16] do not work for the IPUF when x and y are properly chosen.

9.7 Reliability Analysis: Simulation and FPGA Implementation Results

9.7.1 Reliability Analysis of the (x, y)-IPUF with Interposed Bit Position i

We develop the formula for computing the noise of the x-XOR APUF where the noise rate of all APUFs are the same, i.e., all APUFs have a noise rate of $\beta, 0 \leq \beta \leq 1$. Let β_x be the noise rate of the x-XOR APUF. For a given challenge $\mathbf{c}$, if there is an odd number of noisy APUF responses, then XOR APUF's output is noisy. Hence,

$$\beta_x = \sum_{j=0, j \text{ is odd}}^{x} \binom{x}{j} \beta^j (1-\beta)^{x-j} = \frac{1 - (1 - 2\beta)^x}{2}. \quad (23)$$

The equation above is obtained by the following fact: for any given a and b, we have:

$$(a+b)^x - (a-b)^x = 2 \sum_{j=0, j \text{ is odd}}^{x} \binom{x}{j} a^j b^{x-j}.$$

Hence, replacing $a = \beta$ and $b = 1 - \beta$ yields Eq.(23).

Now, we compute the unreliability (i.e. the noise) of the (x, y)-IPUF. We consider the two following cases.

Case I: The output of the x-XOR APUF is reliable. This event occurs with probability $1 - \beta_x$ in which case the noise rate of the output of the IPUF denoted as β_I is equal to the noise rate of the y-XOR APUF denoted as β_y, i.e.,

$$\beta_I = \beta_y = \frac{1-(1-2\beta)^y}{2}. \tag{24}$$

Case II: The output of the x-XOR APUF is unreliable. This event occurs with probability β_x. In this case (see , each APUF in the y-XOR APUF will have noise $\beta' = \beta(1 - \frac{i}{n}) + (1-\beta)\frac{i}{n} = \beta + (1-2\beta)\frac{i}{n}$. Hence in this case, the noise rate of IPUF (denoted as β_{II}) is equal to the noise rate of the y-XOR APUF where all APUFs enjoy the noise rate of β', i.e.,

$$\begin{aligned}\beta_{II} &= \frac{1-(1-2\beta')^y}{2} = \frac{1-(1-2(\beta+(1-2\beta)\frac{i}{n}))^y}{2} \\ &= \frac{1-(1-2\beta)^y(1-2\frac{i}{n})^y}{2} \overset{Eq.(24)}{=} \frac{1-(1-2\beta_y)(1-2\frac{i}{n})^y}{2}.\end{aligned} \tag{25}$$

Therefore, the noise rate β_{II} of the (x, y)-IPUF (denoted as β_{IPUF}) is equal to

$$\begin{aligned}\beta_{IPUF} &= (1-\beta_x)\beta_I + \beta_x\beta_{II} = \beta_y + \beta_x(\beta_{II} - \beta_y) \\ &= \beta_y + \beta_x\left(\frac{1-(1-2\beta_y)(1-2\frac{i}{n})^y}{2} - \beta_y\right) \\ &= \beta_y + \frac{\beta_x}{2}(1-2\beta_y)(1-(1-\frac{2i}{n})^y).\end{aligned} \tag{26}$$

The following examples confirm the correctness of Eq.(26). If $i = 0$, then we have $\beta_{IPUF} = \beta_y$. When $i = 0$, (x, y)-IPUF is basically equivalent to y-XOR APUF. Therefore, the calculated result $\beta_{IPUF} = \beta_y$ makes sense.

If $i = n$ and y is odd, then from Eq.(26), $\beta_{IPUF} = \beta_x + \beta_y - 2\beta_x\beta_y = \beta_x(1-\beta_y) + \beta_y(1-\beta_x) = \beta_{(x+y)-\text{XOR APUF}}$. We do know that when $i = n$ and y is odd, (x, y)-IPUF is exactly the $(x + y)$-XOR APUF. Hence, the calculated result $\beta_{IPUF} = \beta_{(x+y)-\text{XOR APUF}}$ makes sense.

9.7.2 Reliability Simulation of the IPUF and XOR APUF

To compare the reliability of the (x, y)-IPUF to the $(x + y)$-XOR APUF we simulated a $(x + y)$-XOR APUF, (x, y)-IPUF, x-XOR APUF and a y-XOR APUF for $x = 20$, and $y = 2$ and $y = 3$. In the simulation, we have 64-bit APUFs, each with a noise rate defined by setting $\sigma_{\text{noise}} = 0.05\sigma$. To estimate the reliability, we evaluated each PUF design with 10,000 randomly generated challenges. Each challenge is measured 11 times to determine whether it is noisy or not. If the repeatability of a challenge is 100%, we say it is reliable; otherwise, it is a noisy challenge. The reliability of a PUF is estimated as the fraction of reliable challenges.

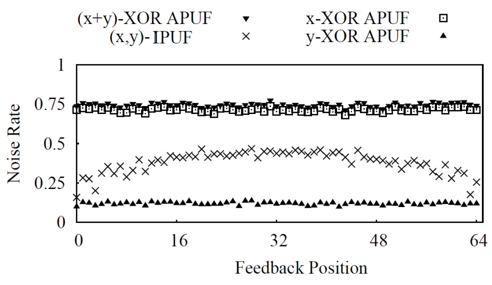

(a) $x = 20$ and $y = 2$

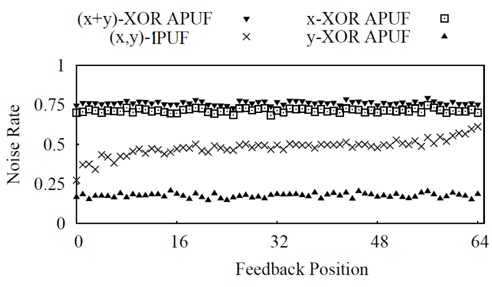

(b) $x = 20$ and $y = 3$

Figure 8: Noise rate of (x+y)-XOR APUF, (x,y)-IPUF, x-XOR APUF and y-XOR APUF when the noise rate of each APUF is around 0.05.

We varied the interpose position i of the IPUF from 0 to 64. For each interpose position we measured the reliability of the (x, y)-IPUF. In the same figure we also plot the reliability of the $(x + y)$-XOR APUF, x-XOR APUF and y-XOR APUF. The simulated results are presented in Fig. 8.

Figures 8a and 8b show that the noise rate of the $(x + y)$-XOR APUF and the x-XOR APUF are close to each other as the value of y is very small compared to the value of x (i.e. $y = 2$ or $y = 3$). The noise rate of the y-XOR APUF is very small compared to the $(x + y)$-XOR APUF and the x-XOR APUF. The noise rate of the $(x, 3)$-IPUF increases when the interpose bit position increases from 0 to 64. However, the noise rate of the $(x, 2)$-IPUF reaches the maximum value at interpose position 32. This is due to the parity of y (see Eq. (19)). The noise rate of the $(x, 3)$-IPUF is equal to half of the noise rate of the $(x + 3)$-XOR APUF when i is in the middle position. The experiments confirm our findings related to reliability (see Section 5).

9.7.3 FPGA Implementation

Reliability of the IPUF with respect to Interposed Position We selected 22 and 23 unique component APUFs to construct a (20,2)-IPUF and a (20,3)-IPUF respectively on the FPGA. We evaluated how the noise rate was affected by changing the interposed positions in the lower XOR APUFs. We tested 5 different interposed bit positions (0, 16, 32, 48, 64). The noise rate of the (20,2)-IPUF and the (20,3)-IPUF with respect to interposed position are shown in Fig. 9. This follows the same trend as the simulation result in Fig. 8. Note that the reliability is equal to (1-noise rate) or (100% − noise rate) in percentage.

Reliability of IPUF under Temperature Variation We used a $(3, 3)$-IPUF for reliability testing under temperature variation, where each APUF is created by random placement, and has good uniformity and uniqueness. We measured 1,000 CRPs from this IPUF under 25 degree Celsius as the reference CRPs. We then measured the same 1,000 CRPs again under 70 degrees and 0 degrees Celsius. The error rate introduced by 70 degrees and 0 degrees Celsius is 2.1% and 1.4%, respectively.

9.8 Enhanced Reliability Based CMA-ES Attack On APUF

In this subsection, we describe enhancements to the original reliability based CMA-ES attack [Bec15]. In the reliability based CMA-ES attack, each model $\vec{w}$ is evaluated according to a fitness function. The fitness function correlates the observed reliability R of the PUF to the reliability of the estimated model R'. Let us denote the observed

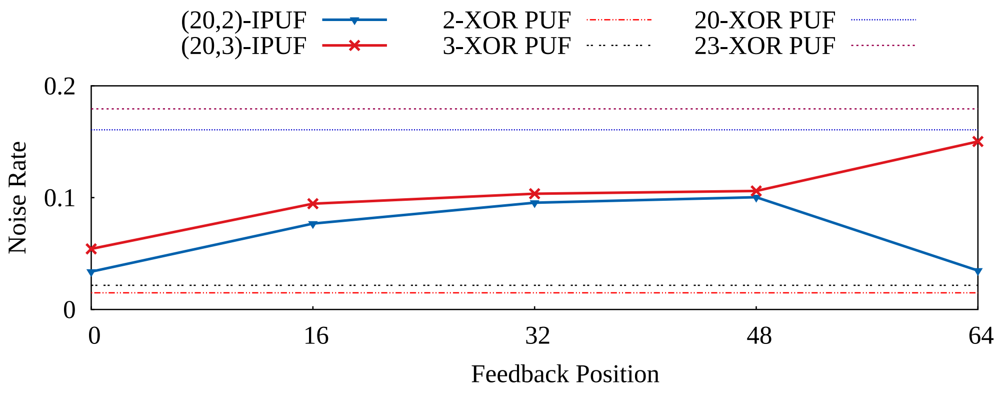

Figure 9: Reliability with respect to different interpose position.

reliability R in Eq. (7) by $R_{original}$ and the model reliability R' in Eq. (8) as $R'_{original}$. The correlation between $R_{original}$ and $R'_{original}$ is limited by the fact that the observed reliability $R_{original}$ only ranges from $[0, M/2]$, while the range of $R'_{original}$ is $\{0, 1\}$. This is significant because the comparison of $R'_{original}$ and $R_{original}$ is not as accurate, since the two terms do not have the same range of values.

We propose two alternative definitions for $(R_{original}, R'_{original})$. We define $(R_{absolute}, R'_{absolute})$ and (R_{cdf}, R'_{cdf}), as follows:

$$R_{original} = |M/2 - \sum_{i=1}^{M} r_i| \quad \text{and} \quad R'_{original} = \begin{cases} 1, & \text{if } |\Delta| \geq \epsilon \\ 0, & \text{if } |\Delta| < \epsilon, \end{cases} \tag{27}$$

$$R_{absolute} = |M/2 - \sum_{i=1}^{M} r_i| \quad \text{and} \quad R'_{absolute} = |\Delta| \tag{28}$$

$$R_{cdf} = \frac{1}{M}\sum_{i=1}^{M} r_i \quad \text{and} \quad R'_{cdf} = \Phi(-\Delta/\sigma_N) \tag{29}$$

We hypothesize that (R_{cdf}, R'_{cdf}) can create a more accurate model than $(R_{original}, R'_{original})$ when attacking an individual APUF for two reasons. First (R_{cdf}, R'_{cdf}) uses the proper reliability ranges. Second (R_{cdf}, R'_{cdf}) takes into account information from two sources: reliability information and the response information of the APUF (by not using any absolute value operation when computing R'_{cdf}). However, when attacking an XOR APUF, the response of each individual APUF is not known so (R_{cdf}, R'_{cdf}) does not improve the reliability based CMA-ES attack in this case.

When attacking an XOR APUF $(R_{absolute}, R'_{absolute})$ outperforms $(R_{original}, R'_{original})$ because it has the proper reliability ranges. It also outperforms (R_{cdf}, R'_{cdf}) because it does not attempt to use any response information (which is not available from individual APUFs in an XOR APUF).

When modeling both APUF and XOR APUF designs, the original reliability based CMA-ES attack can be improved by using more precise fitness functions. This is significant because due to the improved modeling offered by (R_{cdf}, R'_{cdf}) and $(R_{absolute}, R'_{absolute})$, the reliability based CMA-ES attack can now work with less training data, where before the original attack would fail. When sufficient training data is available, the proposed fitness functions give more accurate models than the original fitness function. Table 6 depicts the modeling accuracy of the reliability based CMA-ES attack on a 64-bit APUF. In this set of simulations $\sigma_{\text{noise}} = \sigma/10$, giving the APUF a reliability of around $96 - 97\%$. From Table 6, it is evident that the reliability based CMA-ES attack using our proposed

Table 6: A comparison of 64-bit APUF's modeling accuracy using CMA-ES

$N^{\dagger}$	**Modeling Accuracy(%)**		
	$(R_{original}, R'_{original})$	$(R_{absolute}, R'_{absolute})$	(R_{cdf}, R'_{cdf})
600	60.33	78.27	96.02
1500	69.60	96.64	97.80
3000	97.49	97.65	98.38
6000	97.85	97.98	98.40

† No. of CRPs is used to train a model.

Table 7: Modeling results of 4-XOR APUF using CMA-ES and different reliability models

Model setup	$N^{\dagger}$	**Modeling Acc.(%)**				**Frequency***			
		A_0	A_1	A_2	A_3	A_0	A_1	A_2	A_3
$(R_{o.}, R'_{o.})$	10×10^3	65.10	66.17	67.40	68.96	0	0	0	0
	20×10^3	98.08	97.91	98.23	98.33	1	4	3	1
	30×10^3	98.27	98.06	98.27	98.39	19	10	6	3
	50×10^3	98.31	98.16	98.37	98.44	39	20	17	10
$(R_{a.}, R'_{a.})$	10×10^3	97.53	97.09	97.10	95.24	22	24	31	8
	20×10^3	97.86	97.75	97.74	97.78	24	29	29	17
	30×10^3	98.08	97.89	98.02	98.12	47	27	20	6
	50×10^3	98.17	98.06	98.23	98.27	50	29	16	5

† No. of CRPs is used to train an APUF as well as 4-XOR APUF models.
* No. of correct models (prediction accuracy > 90%) for A_i out of 100 runs of CMA-ES.

model $(R_{absolute}, R'_{absolute})$ and (R_{cdf}, R'_{cdf}) outperforms the reliability based CMA-ES attack using the original model $(R_{original}, R'_{original})$ as proposed in [Bec15]. This is due to both proposed models using the proper reliability ranges. In addition, (R_{cdf}, R'_{cdf}) outperforms $(R_{absolute}, R'_{absolute})$ as both the response polarity and reliability information are considered in (R_{cdf}, R'_{cdf}).

9.9 Enhanced Reliability Based CMA-ES Attack On XOR APUF

To demonstrate the improvement $(R_{absolute}, R'_{absolute})$ offers, we simulated a 4-XOR APUF and ran the reliability based CMA-ES attack 100 times using both $(R_{absolute}, R'_{absolute})$ and $(R_{original}, R'_{original})$. In this simulation each APUF has a $\sigma_{\text{noise}} = \sigma/10$, giving it a reliability of around $96 - 97\%$. The results of this simulation are shown in Table 7. We report two aspects in Table 7: i) modeling accuracy and ii) frequency of the correct APUF models (a correct model has a prediction accuracy greater than 90%). From the results of Table 7 it is clear that $(R_{absolute}, R'_{absolute})$ is able to generate more correct APUF models than $(R_{original}, R'_{original})$. Note that in the case where $N = 10 \times 10^3$, CMA-ES using $(R_{absolute}, R'_{absolute})$ can successfully model all the APUF components but $(R_{original}, R'_{original})$ fails to build any correct APUF models. Our enhancement to the CMA-ES attack results in a more efficient modeling of an XOR APUF.

9.10 Implementation Details

In order to keep the balance between the delays of two competing paths, usually one switch chain is kept in one column of slices on an FPGA. However, in our APUF implementation on a Digilent Nexys 4 DDR with Xilinx Artix-7 embedded [Dig16] there are four LUTs in each slice of the FPGA. Due to the configuration on this hardware, a choice must be made on how to connect the LUTs to form the switch chain. Since the behavior of each APUF is dominated by the routing difference between the two paths, each switch chain must be placed differently for each APUF, in order to create unique APUFs. Note this design strategy only alleviates the uniqueness issue on a single FPGA. If the same bitstream is used to program different FPGAs, the difference of the same APUFs on different FPGAs will be very small. Thus, this is not a general design strategy to improve the uniqueness of APUFs on FPGA, but it is sufficient for us to conduct our experiments.

We have two different ways to place the switch chains: (1) Random placement: we randomly select one LUT in each slice and then connect them together. (2) Pattern placement: we place the switches according to a pre-defined pattern. For example, we only use LUT A and LUT B in every slice. According to our experiments, each design strategy has advantages and disadvantages. For the random placement design strategy, the advantage of this method is that it gives us many options to build unique APUFs. Here we define two APUFs as being non-unique when their responses are the same for more than 60% of the challenges. Initially, we generated 100 different switch chains using random placement. After extensive evaluation, we selected 23 placements of the APUFs, which can provide APUFs with good uniformity (50.2% - 61.6%) and good uniqueness/inter-hamming distance (39.5% - 59.0%). The noise rate of these APUFs under room temperature is between 0.66% and 1.25%. However, with good statistic properties, comes a security weakness in the APUFs. Since the routing between each adjacent switches is randomly selected, there are a few delays that are significantly larger than the other delays. This effectively introduces a few significant weights in the feature vector of this APUF. As a result the difficulty of all machine learning modeling attacks is reduced since only these significant weights need to be precisely modeled (instead of having to precisely learn all the weights). We built the model of individual APUFs to understand the distribution of weights. The standard deviation of the weights of the APUFs created by random placement ranges from 4.23 to 7.48. As we will explain shortly, the standard deviation is much smaller for the pattern placement design strategy, but this method has its own drawbacks.

For the pattern placement design strategy, there are a very limited number of patterns we can generate and some APUFs formed by different placement patterns are not unique. After exhaustively trying 11 patterns[6], we found only 4 placement patterns that can generate 4 unique APUFs. The uniqueness limitation of this design strategy gives us very few options to form an IPUF design with more than 4 APUFs in total. However, the pattern placement design strategy does not have the same security weakness as the random placement design strategy. We also built the model of individual APUFs to understand the distribution of weights in this design. The standard deviation of the weights of the APUFs created by pattern placement ranges from 1.11 to 3.77. Using this design strategy we do not observe the same effect of only a few influential weights (unlike in the random placement design strategy).

9.11 Security Issue Introduced by Careless Implementation

We also used two APUFs created by random placement to form a (1,1)-IPUF with an interposed position exactly in the middle in the lower APUF. Again, we measured 200,000 CRPs with each CRP measurement repeated 11 times to get the challenge reliability measurements. We then sampled a subset of 90,000 challenge reliability pairs out of 200,000 challenge reliability pairs to run the reliability based CMA-ES attack. CMA-ES was able to converge to the model of the upper APUF with 96.6% accuracy. According to our previous analysis and simulation results, only the model of the lower APUF should be built with up to 75% accuracy (i.e., the reliability based machine learning attack on a (1,1)-IPUF is equivalent to the linear approximation reliability based CMA-ES). When CMA-ES converged to the model of the lower APUF, the accuracy was upper bounded by 75%, which confirms our theoretical analysis.

When we discovered the phenomenon of biased weights in the APUFs generated by random placement, we further investigated why this implementation affects the security of

[6] 1 pattern that uses all four LUTs in each slices, 6 patterns that uses a combination of two LUTs in each slices, 4 patterns that uses one LUTs in each slices.

Table 8: Results of the enhanced reliability based CMA-ES attack on (1,1)-IPUF with biased weights.

	SAC	Upper	Lower	Failed
4	0.39	0	10	0
8	0.58	9	1	0
12	0.54	2	8	0
16	0.32	0	9	1
20	0.41	0	10	0

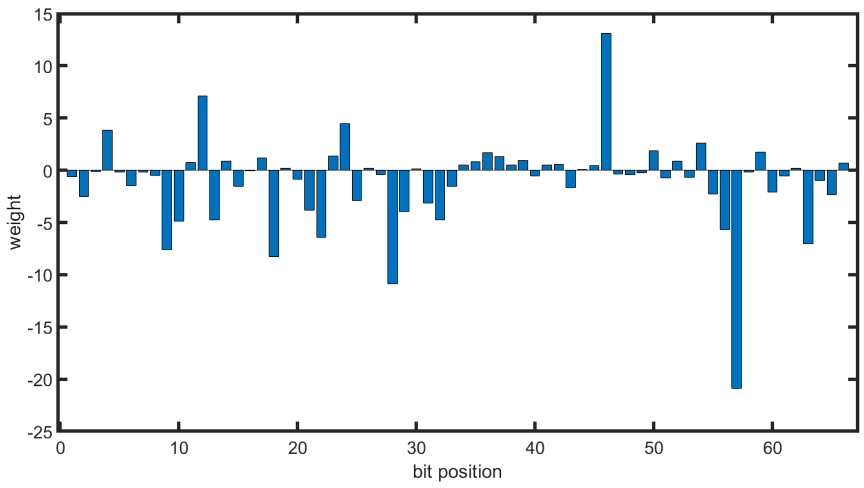

Figure 10: Weights distribution of a lower APUF in one (1,1)-IPUF where the number of large weights (> 3) is constrained to 4.

IPUFs. We created APUF models with biased weights, such that the distribution that generates the large weights is $\mathcal{N}(0,6)$, while the standard weights are drawn from $\mathcal{N}(0,1)$. We also precisely controlled the number of large weights in the second half (the half which is closer to the output) of the lower APUF. We simulated (1,1)-IPUFs with 4, 8, 12, 16, and 20 dominating weights. On each type of IPUF we performed the enhanced reliability based CMA-ES attack 10 times. The results are shown in Table 8.

From Table 8, we can see that the SAC value of the middle bit of the lower APUF will affect its security. The SAC value is computed by the probability that a bit flip in the middle challenge bit of the lower APUF will flip the final output bit. The larger the SAC value is, the higher the chance that the reliability information of the upper APUF will be exposed to adversaries. This leads to a successful attack on the upper APUF with higher probability. Ideally, the SAC value of the middle bit should be 50%, but due to the biased distribution in the weights on FPGAs, the SAC value can be possibly higher than normal. From the computed SAC values, the reliability based CMA-ES attack **is supposed to not** converge to the **upper** APUF because they are good enough to prevent the attack according to our analysis in Section 5.2. However, the attack still works very well when the number of dominating weights is 8 or 12. We can explain this fact as follows. The interposed bit at the middle splits the lower APUF into two parts: the flipping part which is closer to the 0-th challenge bit and the non-flipping part which is closer to the output of IPUF. For the sake of explanation, we assume that all small weights are equal to 0. The motivation of assuming this is that if the biased weights are significant larger than the small weights, we can ignore all the small weights. We assume that there are k biased weights in the flipping part and m biased weights in the non-flipping part. Moreover, the biased weights follow a normal distribution $\mathcal{N}(0, \sigma_b^2)$. From Equation (9), we can write

$$\Delta = (1 - 2\mathbf{c}[n/2]) \times \Delta_{Flipping} + \Delta_{Non-Flipping}$$

where $\Delta_{Flipping} = \sum_{i=0}^{n/2} \mathbf{w}[i] \frac{\mathbf{\Phi}[i]}{(1-2\mathbf{c}[n/2])}$ and $\Delta_{Non-Flipping} = \sum_{i=n/2+1}^{n} \mathbf{w}[i]\mathbf{\Phi}[i]$. Since we have $k + m$ biased weights, $\Delta_{Flipping}$ and $\Delta_{Non-Flipping}$ only depend on k and m weights, respectively. This implies $\Delta_{Flipping}$ and $\Delta_{Non-Flipping}$ follow normal distributions $\mathcal{N}(0, k\sigma_b^2)$ and $\mathcal{N}(0, m\sigma_b^2)$, respectively. We know that, for a given challenge $\mathbf{c}$, the output of the lower APUF would flip by flipping challenge bit $\mathbf{c}[n/2]$ when $|\Delta_{Non-Flipping}| < |\Delta_{Flipping}|$. It is obvious that the smaller $|\Delta_{Non-Flipping}|$ (let's say $< e$), the higher the chance the output will be flipped. Since $\Delta_{Non-Flipping} \sim \mathcal{N}(0, m\sigma_b^2)$,

$$\begin{aligned} \Pr(|\Delta_{Non-Flipping}| < e) &= \Phi(\frac{e}{\sqrt{m}\sigma_b}) - \Phi(\frac{-e}{\sqrt{m}\sigma_b}) \\ &= 2\Phi(\frac{e}{\sqrt{m}\sigma_b}) - 1. \end{aligned}$$

If m increases, then $\Pr(|\Delta_{Non-Flipping}| < e)$ decreases for any given small positive number e. This implies that the leakage of information is reduced when increasing m. This explains why the number of convergences to the upper APUF for case $m = 8$ is smaller than for when $m = 12$. Of course, when m is large enough, the attack does not work. In our simulation, we just need m to be larger than 16 to prevent the attack. In our simulation, we noticed that when $m = 4$, the attack does not work. The weights of lower APUF when $m = 4$ is described in Fig. 10. We give the following possible reasoning. In the non-flipping part, there are two significant large weights and the second largest weight among the two is much smaller (< 13) than the largest one (≈ 23). Moreover, both of them are much bigger than the remaining weights. The smallest value of $|\Delta_{Non-Flipping}|$ is 10 and largest value is 36. This implies that $|\Delta_{Non-Flipping}|$ is always larger than $|\Delta_{Flipping}|$. It means that the leakage of the output of the upper APUF is very small and thus, the attack does not work. Actually in this case, the SAC property for $m = 4$ is 0.39 which is smaller than ideal SAC of 0.5.